Efficiency of Lithium-Ion Battery Energy Storage System

Safa Mahdi Aljabore

Thesis submitted for the degree of
Master in Renewable Energy Systems
60 credits

Institute for Technology
Faculty of mathematics and natural sciences

UNIVERSITY OF OSLO

Spring 2023

Efficiency of Lithium-Ion Battery Energy Storage System

Safa Mahdi Aljabore

Efficiency of Lithium-Ion Battery Energy Storage System

http://www.duo.uio.no/

Printed: Reprosentralen, University of Oslo

Preface

This master's thesis is the final part of the Renewable Energy System Master's degree program at the Department of Technology Systems (ITS), University of Oslo (UiO). This thesis is in collaboration with Institute for Energy Technology (IFE). The aim of this research is to develop a methodology for finding battery system efficiency from operational data. The operational data is based on a battery system connected to a photovoltaic system located in Viken, Norway. First and foremost, I would like to extend my thanks to my supervisors from IFE, Erik Stensrud Marstein and Jonathan Fagerström, for guiding me patiently through the entire process and providing me with useful advice on how to approach this subject. I would also like to thank Ola Johansson and Tore Filbakk from Solcellespesialisten for providing me with details and answers regarding the specifications of the battery system. Additionally, I would like to express my appreciation to IFE and ITS faculty for providing me with all the necessary resources in order to realize this research. Lastly, I would like to express my appreciation to friends and colleagues who provided me with constructive feedback and support throughout this journey.

Abstract

Incorporating electrical energy storage with intermittent renewable energy technologies will increase their availability. To provide insight on the performance of battery storage systems as well as potentially reduce maintenance costs, a real-time performance evaluation of the battery system is required. Although operational data can potentially be used for performance monitoring of the battery systems, there is currently a lack of research on the real-time performance of battery systems in solar photovoltaic plants. One suggestion to accommodate this is to provide a methodology for performance evaluation through operational data by calculating the system efficiency. While the efficiency of battery systems has previously been discussed, it was mostly based on simulated systems. The aim of this thesis is to explore the possibilities of monitoring systems for the performance analysis of battery storage systems, with a particular focus on system efficiency. The approach in this study involved identifying and utilizing relevant influencing factors to perform system efficiency calculations. The findings indicated that the calculated system efficiency was contingent on various factors, both in terms of data quality and operational impact. To achieve consistent results, these factors had to be considered. Based on these findings, the study suggested a methodology for calculating system efficiency that involved consideration of the "state of charge"-difference, missing data and resolution for data quality and energy input, the average "state of charge", and the idle period for operational impact.

Contents

List of Figures

List of Tables

List of Acronyms

AC Alternating Current.

Ah Ampere hours.

BESS Battery Energy Storage System.

BMS Battery Management System.

CCV Closed Circuit Voltage.

DC Direct Current.

DOD Depth of Discharge.

EMS Energy Management System.

EOL End of Life.

ESS Energy Storage System.

EV Electric Vehicle.

IEC International Electro-technical Commission.

LCO Lithium Cobalt Oxide.

LFP Lithium Iron Phosphate.

Li-Ion Lithium ion.

LMO Lithium Manganese Oxide.

LTO Lithium Titanate.

MWh Mega Watt hours.

NaN Not a Number.

NCA Nickel Cobalt Aluminum Oxide.

NMC Nickel Manganese Cobalt Oxide.

NREL National Renewable Energy Laboratory.

OCV Open Circuit Voltage.

POC Point of Connection.

PR Performance ratio.

PV Photovoltaic.

RE Renewable Energy.

RTE Round Trip Efficiency.

SOA Safe Operating Area.

SOC State Of Charge.

SOH State of Health.

TMS Thermal Management System.

VRE Variable Renewable Energy.

Wh kilo Watt hours.

Introduction

1.1 Background

Due to climate and energy security concerns, the current focus in the energy sector is on incorporating clean energy into the market. Two examples of plans that provide incentives for transitioning from conventional energy production to clean energy production, through renewable energy (RE), are the UN-NET zero emission goal and REPowerEU. The first aims at limiting global warming to a maximum of 1.5 degrees $^{\circ}C$ compared to pre-industrial levels [1], and was presented as a part of the United Nations' Sustainable Development Goals. The second plan was launched by the European Commission in response to power supply uncertainties in Europe caused by the Russian invasion of Ukraine. Their aim was to emphasize diversifying energy supply, reducing energy consumption, and producing RE to increase energy security [2]. In order for RE to compete with conventional electricity generation, it must reach a certain level of availability. This poses a particular challenge for Variable Renewable Energy (VRE), a RE technology unable to independently provide a constant and flexible power supply. One example of VRE technology is photovoltaic (PV), which utilizes the properties of semiconductors and solar radiation to generate electricity and has the advantage of relying on a globally available resource. However, the variable nature of solar radiation makes the quality and quantity of PV electricity production intermittent. To optimize energy efficiency, PV is increasingly being installed in hybrid systems with an energy storage option. One application of an Energy Storage System (ESS) in PV is to prevent energy wastage during peak production hours when surplus PV production exceeds the load. In that case, excess PV production is stored in the ESS for later use, thus improving overall system availability. Figure 1.1 illustrates the functionality of a PV-ESS hybrid system.

1.2 Battery Energy Storage Systems

Electrochemical ESS, which uses batteries, is referred to as a Battery Energy Storage System (BESS) and is defined as a technology that has the ability to store electrical

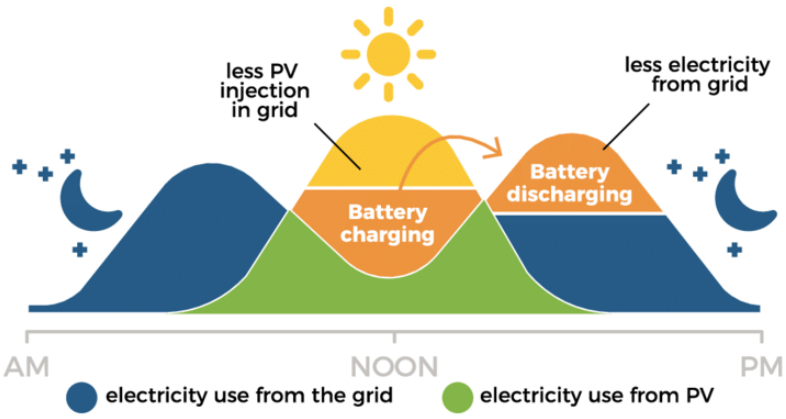

Figure 1.1: Example of an application of a hybrid system with BESS and PV. The figure illustrates how BESS acts as storage for surplus PV production in periods with surplus demand (Source: [3])

energy for later use [4]. The most relevant battery technologies used in BESS, in terms of market size, are Lithium-ion (Li-ion) and lead-acid batteries. Lead acid was the first established battery technology with a cheaper installation cost, and Li-ion technology was very attractive due to its high energy density, allowing it to store large amounts of electrical energy in smaller volumes. In previous years, Li-ion technology was held back by its high installation costs; however, recently, these prices have declined [5, 6] and allowed Li-ion technology to occupy a larger part of the battery market. According to [7], the 2021 global battery market size was mainly represented by Li-ion and lead-acid technologies, as illustrated in Figure 1.2. Li-ion technologies are also extensively used

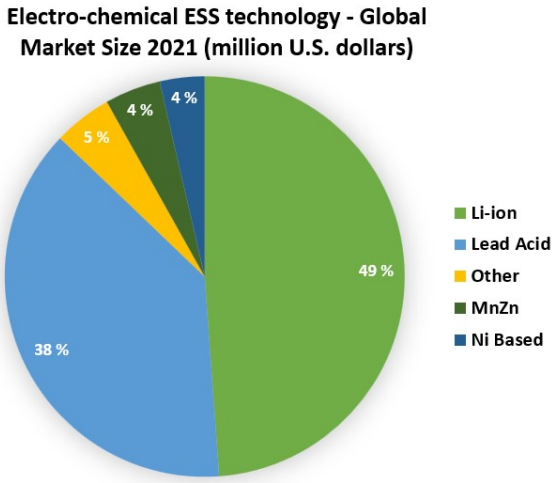

Figure 1.2: A pie chart that represents the market size for different battery technologies as BESS. The market size was given in millions of U.S. dollars. The data was last updated in 2021. The pie chart shows that Li-ion and lead acid were the dominant technologies in the market. (Source: [7])

in the research field. A study that aimed to provide a review of BESS technologies concluded that Li-ion batteries are the dominant technology in stationary applications due to their high energy density, energy efficiency, and depth of discharge (DOD) [8]. A study that conducted linear optimization for battery selection [9], stated that, due to the mentioned properties, Li-ion batteries are the most cost-effective option for BESS applications. This made them suitable for a diverse range of applications [10, 11] and allowed them to become the most established technology in both the market and the research field.

The BESS can be enhanced by either improving the technology itself or by optimizing its usage. The improvement of BESS through optimizing its operational behavior involves conducting safety and performance testing. Safety testing is to ensure the safety of the BESS under an operation, while performance testing is to evaluate the BESS's ability to perform its intended function effectively. Standards for safety testing on BESS have been well established internationally, but according to [12], there is a lack of standards related to the performance testing of stationary BESS.

1.3 Performance Testing

In 2021, the National Renewable Energy Laboratory (NREL) published the "Global Overview of Energy Storage Performance Test Protocols" [12], which provided a list of existing standards related to performance testing for BESS. They started with an overview of available standards for performance testing of BESS worldwide, with many national standards referencing the International Electrotechnical Commission (IEC) standards. They identified "IEC 62933-2-1: Unit parameters and testing methods" as the main standard related to performance analysis in BESS [13]. The report concluded that while most IEC standards provide extensive protocols for performance testing, they are primarily focused on Electric Vehicle (EV) batteries and mobile devices and highlighted that there is a lack of standards available for large-scale BESS and their use cases. Additionally, performance testing is typically executed with test data, which is created to simulate real-life operational data with the purpose of recreating operational conditions that may occur under different scenarios. The report also provided a database for an international collection of available test data.

The relevant IEC standard [13] suggests methods for parameter testing and provides specifications for test conditions to ensure consistent testing of BESS properties. Their testing approach requires BESS to be in a controlled environment where conditions can be specified according to which type of test is performed. The standard suggests one method, called the "back-to-back' test, where BESS doesn't have to be physically

disconnected during testing. The back-to-back test is when a test module is connected between the test subject and an external power source, such as the grid, that generates desired voltages and currents, creating a controlled environment for the test subject without physically disconnecting it. This still implies that the BESS is unavailable during testing.

When evaluating the performance of BESS, it is important to select the appropriate parameters. The report by NREL [12] identifies that the most commonly used parameters for performance testing are capacity fade, both in operation and storage, and system efficiency, including both charge efficiency and energy efficiency. Where the system efficiency is found by calculating the Round Trip Efficiency (RTE), the IEC standard [13] also suggests other parameters such as input/output power ratings, expected service life, system response, auxiliary power consumption, self-discharge, voltage, and frequency ranges. Regardless, RTE is the most commonly used performance evaluation parameter for finding BESS efficiency. Not only does it provide the actual energy losses, but it also requires simple metrics that depend on accessible measurements.

1.3.1 Studies on System Efficiency Analysis

Recent studies that have explored BESS efficiency include "Energy efficiency evaluation of a stationary lithium-ion battery container storage system via electro-thermal modeling and detailed component analysis" [14] by Schimpe, where they map out 18 loss mechanisms related to a BESS in three different application scenarios. Another study is "BESS modeling: investigating the role of auxiliary system consumption in efficiency derating" by Rancilio, which explored different factors that impact the final RTE by providing a range for each input value in their calculations. However, these analyses were executed using simulated data. This suggests that there is currently a research gap in the field regarding the performance evaluation of BESS through actual operational field data. This research will therefore investigate aspects of BESS performance through operational data to both examine conclusions from existing literature and possibly find new cases that emerge during the operation of a BESS in a real-world system.

1.4 Motivation

1.4.1 The Need for Performance Analysis on PV and BESS Hybrid Systems

The current methods for performance testing of BESS rely on test data or specific BESS usage scenarios. Since it is expected that operational conditions during testing will vary, these performance test will not always be representative of the actual performance. While monitoring systems provide some information about the battery's condition during BESS operation, they provide simple measurements and estimations of its state and health, not a comprehensive evaluation of the BESS's performance. This shows that there is a need to develop performance evaluation methods based on operational data in order to enable convenient maintenance without disrupting BESS operation and provide more insight on the BESS's performance quality. A recent paper [15] conducted an interview with 100 PV owners regarding the barriers to investing in a BESS for their PV system. PV owners were hesitant to invest, despite knowing the advantages of a PV-BESS hybrid system. The results showed that the main barriers were related to concerns about the performance of the BESS, specifically the risk of deterioration over time and the risk of poor performance, followed by concerns related to investment costs. Other studies have explored these barriers, and various strategies have been proposed to improve BESS cost efficiency. For example, [16, 17], suggested that it is possible to maximize profits, by either favoring specific applications or utilizing multiple applications simultaneously. However, there is a lack of studies regarding increasing the reliability of BESS technical performance during operation.

1.4.2 Experience from Performance Analysis of PV Systems

The performance evaluation of PV systems through operational data has progressed significantly compared to that of BESS. Understanding relevant experience in this matter could be beneficial in determining a starting point for this research. The main performance parameters for PV systems are energy yield and Performance Ratio (PR), but estimating these parameters is challenging due to variations in operational conditions and data processing issues [18, 19]. The solution involves identifying non-physical data, missing data, and unexpected measurements. In terms of operational conditions, the IECTS61724-3 standard for PR measurements requires specific conditions for the systems in order to achieve consistency. This is because the performance evaluation of PV is contingent on the characteristics of the power input, where the main factors are environmental conditions, which determine the quantity of solar radiation, cloud cover, and ambient temperature. Typically, only acceptable operation are included in

the PR analysis; this is to differentiate between faulty and acceptable performance. The main takeaways from experience in PV performance analytics are the emphasis on assessing data quality, considering specific functionality, and defining acceptable performance. This illustrates that assessing the quality of the BESS data before using it in analysis is crucial. The BESS is similar to PV in terms of contingency on specific functionality, and including this property in the discussion on performance analysis is important.

1.5 Considerations When Evaluating the Performance of BESS

When conducting performance evaluations, it is important to take into account the specific context in which the BESS is utilized. This approach is already established in the standard regarding parameter testing [13], where efforts are made to classify applications before defining performance metrics. BESS applications are classified into three categories, which are based on the duration of a full cycle. These categories include short-duration applications ($<$ 1 hour), such as frequency regulation, and long-duration applications ($>$1 hour), such as peak shaving, and backup storage. It should be noted that the definition of when an application transitions from long-duration to back-up storage has not been specified. Other studies, such as [11], categorized applications based on the power rating, where large-scale BESSs are rated at $>$ 100 MW, medium-scale BESSs are rated between 5 and 100 MW, and small-scale BESSs are rated at $<$ 5 MW. Small-scale BESSs typically range from 13.5 kWh for residential customers to 10 MWh for commercial and industrial units.

Specific applications when attempting to examine the efficiency of BESS are typically either peak shaving, which is used as an example of a long-duration application, or frequency regulation, which is used to represent a short-duration application. Peak shaving involves storing excess energy during periods of low demand and utilizing it during high-demand periods and is used for economical profits, while frequency regulation is a grid support service that ensures electricity supply and demand balance at all times and requires low response times, typically in the range of seconds [20]. These scenarios are used to examine two different operational conditions for the battery. Specifically, peak shaving exposes the BESS to low-frequency but high-intensity energy requests, while the frequency regulation application subjects the BESS to frequent low-intensity energy requests throughout the relevant time period [21].

1.6 Scope of Work

1.6.1 Objective

The objective of this research is to explore the possibilities of monitoring systems for the performance analysis of BESS, with a particular focus on system efficiency. By using operational data, the study will showcase calculated system efficiency and propose a method for evaluating the performance of BESS.

1.6.2 Scope

The scope of this work will focus on the performance and durability of an operational Li-ion BESS and is restricted to an analysis of the technical performance of Li-ion BESS. Since the system boundaries will be limited to the performance of the entire BESS and its subsystems, which include the battery pack, usually comprised of several battery cells connected in series or parallel, power electronics, which include the converters, and auxiliary systems, which include the control systems and thermal management systems. Although the performance of the battery cell is important to evaluate the durability and lifetime of the battery, the total performance of the battery subsystem is more representative when evaluating the functionality of BESS, the performance of a battery cell alone will not account for BESS efficiency. Although the auxiliary system is not included in the calculations due to limited available information, it will still be a part of the discussion in the chapter on the theoretical background. The data used for analysis is collected from BESS monitoring systems, referring to sensors that monitor functional parameters such as voltage, current, and temperature within the battery pack and the BESS at the point of connection. Although both long- and short-duration applications are mentioned in the discussion on BESS efficiency in the theoretical background chapter, the specific functionality for the actual analysis will be restricted to peak shaving-related applications, also categorized as long-duration applications. The test procedures for determining the performance parameters of a BESS are generally carried out under controlled conditions, which requires taking the BESS offline during the testing period to achieve high accuracy results. The innovative aspect of this research is the attempt to perform continuous performance analysis using operational data. If the accuracy of analysis through operational data is comparable to that of standard test procedures, it may be possible to replace the need for performance tests, potentially reducing operational and maintenance costs.

1.7 Structure

In Chapter 2, the theoretical background is presented, including relevant theories and literature on the properties and loss mechanisms. The first section will present existing literature and the properties of BESS. Then, each subsystem within BESS will be presented similarly, starting with the power conversion subsystem, followed by the battery subsystem, and finally the auxiliary subsystem. In Chapter 3, the methodology presents the strategies and models that are utilized to obtain the results. Firstly, the actual data used for the analysis will be presented, followed by a discussion of different aspects related to the data and the cleaning process. The calculations on system efficiency will also be presented. In Chapter 4, the results will show the outcomes of the strategies described in the methodology section. The findings are summarized in a section that describes a suggested methodology for calculating system efficiency. A discussion related to each result will be presented immediately after the results, followed by a final discussion at the end. Chapter 5 concludes with a summary of the findings and suggestions for further research.

Theoretical Background

The battery efficiency is a variable, subject to the effects of its unsteady-state properties. Measuring the BESS efficiency adds another layer of complexity, as losses in other subsystems must be included, such as losses arising from power electronics and auxiliary subsystems. Section 2.1 begins by discussing BESS efficiency and related loss mechanisms in order to identify factors contributing to losses within the system. Sections 2.2, 2.3, and 2.4 goes into further detail on the loss mechanisms and the related influencing factors for each component. Finally, Section 2.5 provides an overview of the findings related to these factors.

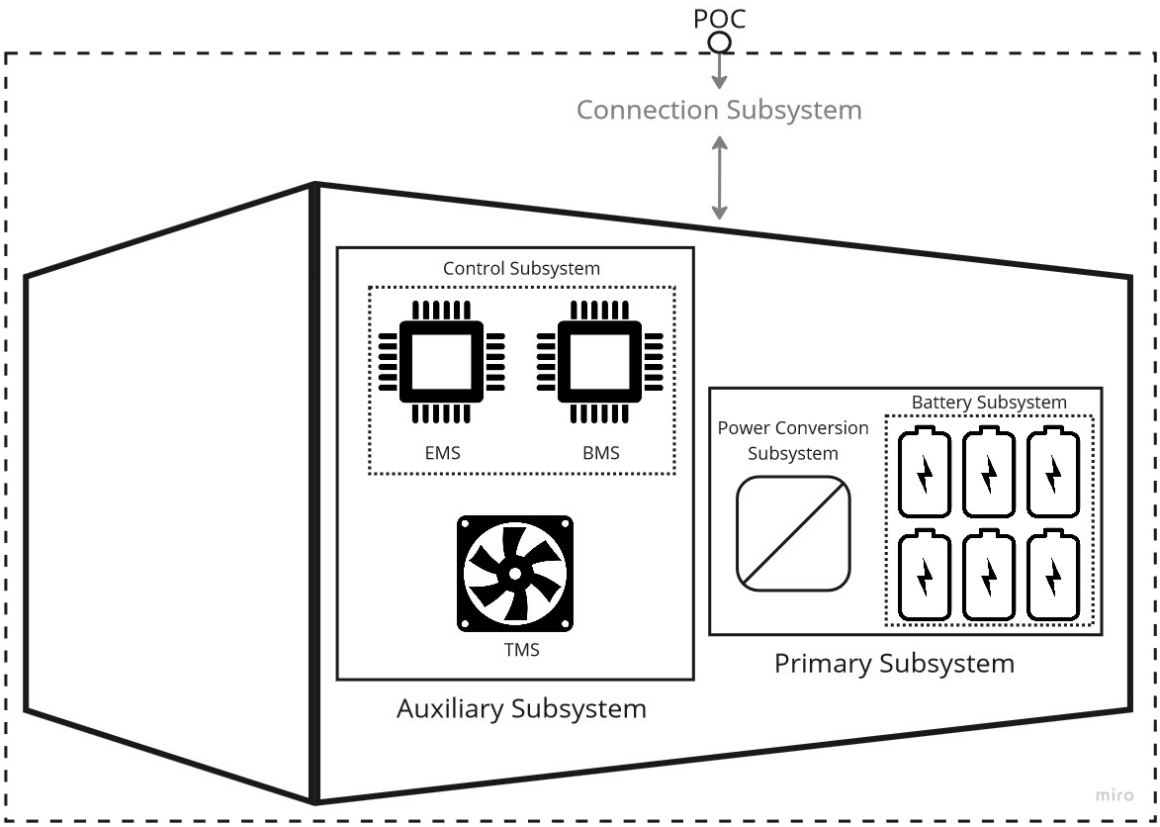

Figure 2.1: A demonstration of different components within the BESS, where the gray part is considered out of scope for this project.

2.1 Battery Energy Storage System

In order to enable a thorough discussion, the subsystems of BESS must be defined. BESS is typically divided into three primary subsystems: the battery subsystem, which includes the entire battery pack; the power conversion subsystem, which includes the power electronics responsible for converting current; and the auxiliary subsystem, which includes control and management systems such as Energy Management System (EMS), Battery Management System (BMS), and Thermal Management System (TMS) [21]. The international standard for parameter testing [13] additionally includes the connection subsystem as a part of the system boundaries. They also provided two possible typologies: one where the auxiliary power consumption is provided by the battery, thus contributing to energy losses at Point Of Connection (POC), and the second where the auxiliary power consumption is provided by an external power source. Figure 2.1 provides a simple sketch of a BESS, using the system boundaries provided by [13], where the subsystem in gray is considered out of scope for this research. The placement of POC is also found in Figure 2.1.

2.1.1 Important Metrics

Before discussing BESS efficiency, important metrics need to be defined, such as rated power, BESS efficiency, RTE, and actual capacity. The rated power is the maximum constant power that can be achieved at the POC under standard conditions, with the duration specified [13]. They classified rated power into three categories: active power [W], reactive power [var], and apparent power [VA]. For this research, only active power is considered. Energy is the product of power and time [h], with a unit of watt-hours [Wh]. BESS efficiency is referred to as the system efficiency, and the RTE is the calculated system efficiency, which is the ratio of energy output to energy input measured at POC, expressed as a percentage between 0% and 100%. The resulting percentage reflects the energy losses that occurred between these two events. Lastly, the actual capacity of a BESS refers to the maximum energy output at the POC when the battery is discharged between the maximum to minimum State Of Charge (SOC) and is the product of the maximum energy output and the discharge time period, [13]. When referring to the actual capacity of BESS, the conversion losses and power consumption from the auxiliary subsystem are accounted for. It is required that the BESS is discharged with a constant C-rate and measured under standard conditions to ensure consistent results.

2.1.2 Battery System Efficiency

A higher BESS efficiency is typically used to describe a process that accomplishes the same task while consuming less energy and is related to lower energy losses. This means that decreasing the energy losses in a process will increase its efficiency. According to [13], the BESS efficiency depends on its actual capacity, rated power input and output, power consumption of auxiliary subsystems, and standard testing conditions.

In addition to the IEC standard [13], there are also research studies that have attempted to provide insight on the influencing factors related to BESS efficiency. The study [22] found that the efficiency of BESS depends on the power input, SOC range, and auxiliary power consumption. They categorized the losses into losses due to operational effects (i.e., losses in batteries and inverters) and the power requested by the auxiliary system. Another study by [14] defines the final efficiency of a BESS based on an application scenario. They conducted simulations for both short- and long-duration application scenarios and analyzed loss mechanisms, including losses of conversion and losses due to auxiliary system consumption. The study [21] focused on the efficiency loss due to power conversion and the battery. They suggested that the efficiency of power electronics and batteries plays a significant role in the overall efficiency of the system. In terms of the battery's role, according to [8], the absolute efficiency value depends on the SOC level, charge and discharge rates, idle period, and temperature, which will be further discussed in the following sections.

2.2 Power Electronics

Power electronics refers to converters that allow current flow between systems with different types of current. For example, the current in the BESS and PV module is direct current (DC), and the current in the grid and load site is alternating current (AC), and if the PV wants to deliver current to the grid, then it requires converters. There are two types of converters: an inverter and a rectifier. An inverter is used to convert DC to AC, such as in PV-to-grid or battery-to-grid cases. An AC-to-DC converter is called a rectifier and is used, for example, in grid-to-battery. Converters also have a maximum capacity, which is important to consider when choosing a suitable converter for the BESS. Since the BESS will never exceed its maximum capacity, choosing appropriate converters is a simple process.

2.2.1 Switching, Conducting and No-load Current

There are three types of losses in converters, switching, conducting and no-load current. If the inverter is connected in a circuit, there will be a small current flow even when

no load is applied, which is known as 'no-load current', 'standby power supply' [23] or also called 'idle power'[24]. When there is no load on the inverter, the inverter will go into standby mode, where it will still consume power to maintain memory and control circuit functions. This means that when the inverter is in standby, its efficiency is significantly lower than when a load is applied [24]. The relevant efficiency curve is typically provided by the manufacturer and shows how the efficiency varies depending on the load. To avoid the no-load current, it is possible to include an 'automatic switch' that requires a lower-limit power supply in order to switch on. The issue here is that if the power supply is less than the threshold, the inverter will fail to switch on and cause inconvenience; therefore, it is preferable to use the 'constantly on' feature. Other losses in the converters are due to switching and conduction. The switching losses in an inverter are related to the change of state of the device (on or off). The conduction losses depend on the voltage-current characteristics of the electronics [25]. In order to avoid switching losses and improve the efficiency of a power inverter, the switch count (turn-on/off) needs to be taken into consideration, and the losses will therefore typically vary depending on the type of application. The study, [21] illustrated a BESS where the system boundaries include battery and power electronics while disregarding the auxiliary system consumption. Their results showed that the conversion losses in frequency regulation applications account for almost all losses, while in peak shaving applications they account for almost equal parts of battery losses. This can be explained by the fact that frequency regulation requires frequent switching and higher loads. Additionally, higher temperature will also cause an increase in conduction and switching losses [25].

2.3 Battery

The term "battery" refers to a battery pack consisting of multiple battery cells that are connected either in series or parallel. The battery technology used in this context is Li-ion, and the characteristics of different commercially available Li-ion technologies have an impact on efficiency in diverse ways, which is why a description of these technologies is included. The battery's energy efficiency is evaluated based on its voltaic and coulombic efficiency, which are discussed separately. During operation, the primary causes of energy loss are usually internal losses and overvoltages. Furthermore, the degradation of the battery due to cycle aging and calendar aging is also addressed.

2.3.1 Important Metrics

Important metrics to know before discussing efficiency are voltage, current, power, C-rate, SOC, cycle, and capacity. The voltage is measured in volts [V] and is the

potential electrical energy in a circuit. The open circuit voltage (OCV) is the voltage of the battery when there is no current flow from external sources [26] and when the battery cells are in chemical equilibrium. The Closed Circuit Voltage (CCV) is the voltage during operation when the battery is connected to a circuit. The rated voltage V_{Rated} gives the range of safe operating voltages for the battery and is defined as $V_{Nominal} \pm 10\%$. The operating voltage, or working voltage, is the range of voltage when the device is under operation, i.e., charging or discharging. For normal operation, it is expected that the battery operates within the range of the rated voltage. Cut-off voltage, refers to the minimum voltage at which a battery is considered fully discharged, beyond which further discharge can potentially cause damage. This voltage level is typically chosen to ensure that the maximum useful capacity is reached. The nominal voltage V_{Nom}, is usually used to describe the average or normal operating voltage of the battery. According to [27] the $V_{Nominal}$ is determined as the voltage of the battery when discharged halfway between the fully charged state and the end voltage at which the battery spends most of its time. $V_{Nominal}$ at the beginning of life is specified by the manufacturer or supplier of the battery.

Voltages in the battery generate electrical current, i.e., the flow of electrical energy, and is measured in amperes [A]. The operating current is the range of possible currents during operation. Both the voltage and current range of a battery are determined by the chemistry and design of the battery cell. Charge, with a unit of ampere hours [Ah], is the product of current and time and is used to describe the amount of electrical energy stored in the battery. Power is the voltage multiplied by the current and describes the energy flow as a product of current and voltage.

$$P = V \times I$$

Where P is the power, V is the voltage, and I is the current. Power is proportional to current and voltage, and an increase in either will result in higher power. The battery efficiency is the ratio between the output and energy input of the battery.

The C-rate is a measure of the speed of charging or discharging the battery. For example, charging at a C-rate of 1C means that the battery is charged from $0 - 100\%$ in one hour. The definition of C-rate is the charge/discharge current divided by the nominal capacity, C_{nom}

$$C - rate = \frac{I[A]}{C_{nom}[Ah]}$$

To illustrate this, if the current is 200 A and the capacity is 200 Ah, then the C-rate is equal to 1. SOC is the level of charge stored in the battery relative to its actual maximum capacity. This value is typically expressed as a percentage, where 0% indicates that the battery is fully discharged and 100% indicates that the battery is fully charged. It is common to limit the battery's SOC to avoid a fully charged or fully discharged state. Therefore, the effective SOC range refers to the actual possible SOC range after restriction. Another important term that needs to be defined is "cycle". One cycle is discharging the battery from 100% to 0% and charging it to 100% again. If the battery doesn't fully discharge or charge, then it is referred to as a "partial cycle". The capacity of the battery is the maximum possible energy discharged from the battery. It can be given in either Ah, representing the charge capacity, or Wh, representing the energy capacity. There isn't any standardization of the different terms for capacity, but here is an attempt to summarize the most common ways to refer to the capacity of the battery. nominal capacity, rated capacity, installed capacity, maximum capacity, or maximum effect is how many Ah or Wh the battery can provide under specific conditions and is usually provided by the manufacturer at the beginning of life. The usable, effective, or actual capacity is the capacity that the battery is actually able to deliver.

2.3.2 Different Technologies

The selection of a suitable battery technology is a critical factor for BESS efficiency. There are five primary commercially available cathode chemistries for BESSs: Lithium Cobalt Oxide (LCO), Nickel Cobalt Aluminum Oxide (NCA), Lithium Manganese Oxide (LMO), Nickel Manganese Cobalt Oxide (NMC), and Lithium Iron Phosphate (LFP). These chemistries are typically paired with a graphite anode material. There is one additional technology that is identified by the anode chemistry, which is Lithium Titanate (LTO). In estimating the properties for each technology, the studies [20, 28, 29] uses general assumptions to provide a comparison between the characteristics of each technology, such as the specific energy, cycle life, cost, and growth potential. A summary of their findings is presented in Table 2.1. The specific energy is a measure of the battery's energy density. The cycle life provides an estimate of the battery's lifetime, with one cycle being defined as one full charge and discharge of the battery. It is important to note that this number is used for comparison purposes and will vary depending on the operating conditions of the battery. Finally, the cost refers to the installation cost (2016) of the technology, while the growth potential indicates the projected market growth of the technology.

Currently, pure LCO batteries are less common due to the high cost of cobalt. In-

Battery Chemistry	Acronym	Application	Specific Energy $\frac{Wh}{kg}$	Cycle Life	Cost$[\frac{\$}{kWh}]$	Marked Growth potential
		Small				
LiCoO2	LCO	Portable Electronics	150-200	500-1000	-	Not relevant
LiNiCoAlO2	NCA	EV (TESLA), Storage, Other	200-260	500-1000	350	High
LiMnO2	LMO	Medical Dev.	100-150	300-700	-	Limited
$LiNi_{0.33}Co_{0.33}Mn_{0.33}O2$	NMC/NCM	EV, Storage, Other	150-220	1000-2000	420	High
LiFePO4	LFP	EV, El-Bus, Storage	90-120	>2000	580	Moderate
Li2TiO3	LTO	EV (Mitsubishi, Honda), Other	50-80	3000-7000	1005	Moderate

Table 2.1: Li-ion cathode chemistry and their properties for commercialized technologies with graphite anodes.

stead, NCA (a version of LCO) is more commonly used, as it requires less cobalt and is more thermally stable [28]. Although NCA has the highest specific energy among the technologies listed in Table 2.1, its major drawback is safety-related. LMO was developed as a cheaper alternative to LCO by substituting cobalt with manganese. However, its cycling performance was still unsatisfactory, leading to the development of NMO and later NMC, which aimed to enhance structural stability. Researchers also investigated different structure types, leading to the development of LFP, known for its thermal stability and high power capability but with the lowest specific energy among the technologies mentioned in Table 2.1. The most relevant Li-ion technologies today are NCA, NMC, and LFP. With NCA and NMC offering high specific energy and LFP offering high cycle life and independence from cobalt. According to [5], as of 2017, NMC represented 53% of the global market size for EV batteries, while NCA represented 46%, with the remaining portion being LFP. However, this did not include China, which primarily relied on LFP technologies. In the electric bus market, LFP is the dominant chemistry in China, with 88% of electric buses utilizing LFP batteries in 2018 [30]. Since LFP suffers from low energy density and slow charging rates compared to NMC, it is expected that NMC will eventually gain market share in this segment. LTO is typically used for heavy-duty applications due to its ability to extend cycle life and is considered the safest battery technology. However, its high cost may limit its market growth potential.

A study conducted by [31] found that NCA and NMC batteries have an RTE 6% higher than LFP when used for battery storage. However, LFP has an advantage over the other technologies in terms of low material costs. Another study by [21] compared 350 kWh NMC and LFP batteries in peak shaving applications and found that losses were slightly higher with LFP for both new and aged cells. On the contrary, a study by [8], conducted experiments for three different applications on LFP and NCA batteries. The study found that the highest degradation in capacity for LFP was during frequency regulation applications, while for NCA it was highest during peak shaving. The study concluded that LFP cells have better capacity, energy, and efficiency retention for calendar aging, cycle life for peak shaving application. NCA cells have

higher stability with respect to capacity and energy retention for frequency regulation applications. This illustrates how the difference in battery efficiency between the two chemistries varied depending on the application. In conclusion, the choice of technology should be suited to the type of application to optimize efficiency and cycle life.

2.3.3 Battery Efficiency

The concept of energy efficiency in batteries is the product of voltaic efficiency and coulombic efficiency, [32]. The coulombic efficiency represents the ratio between the charge removed during discharge and the charge required to restore the initial capacity [20]. It is commonly used to evaluate the irreversible capacity loss due to irreversible chemical reactions inside the cell. And the coulombic inefficiency can be used as an indicator of the loss of lithium ions for each charge and discharge cycle.

The voltaic efficiency is the ratio between the average voltage during discharge and the average voltage during charge. Typically, the voltage required for charging a battery is higher than that required for discharging it, and the difference between the discharged voltage and charged voltage is a reflection of the voltaic inefficiency of the battery. Studies have shown that high C-rates can lead to greater voltaic inefficiency, resulting in lower overall efficiency [32]. This is because high C-rates cause the operating voltage $V_{operating}$ to deviate further from the OCV, leading to higher overvoltages [33]. The concept of overvoltage will be discussed in more detail in the following sections.

2.3.3.1 Internal Resistance

According to Ohm's Law, the internal resistance of a battery, R, is directly proportional to its power, P.

$$R = \frac{P}{I^2}$$

This indicates that given a constant current, an increase in power will cause an increase in internal resistance for both charging and discharging, which leads to energy losses, which are either dissipated as heat or induce unfavorable chemical reactions within the battery cell [34]. Since power is dependent on voltage, this equation highlights how higher voltages can lead to greater energy losses, as indicated by the relationship between power and internal resistance. According to literature, the efficiency of the battery is determined by its operational conditions. The main factor is the C-rate, and whether the battery is charging or discharging. A study, [35] estimated that the RTE of the battery was 97% while charging and 95% while discharging for C-rate of

≤ 1. Higher C-rates represented more stress on the battery and lower RTEs, which is also illustrated in [21, 34] where they demonstrated the impact of different C-rates on total losses. They found that high C-rates resulted in higher internal resistance, which was related to greater energy losses. Other factors related to internal resistance are the SOC levels of the battery. A study conducted by [36] investigated the relationship between C-rate, SOC, and DOD levels on battery health and concluded that both high and low SOC levels contributed to higher internal resistance, although high SOC levels had a greater impact than high C-rates. Studies, such as [14] who investigated the relationship between SOC and cell resistance during both charging and discharging, found that excessively high or low SOC levels lead to increased internal resistance and energy losses. The study [21] observed a similar trend between SOC and OCV, and discusses the impact of SOC level on internal resistance.

2.3.3.2 Overvoltage

Overvoltage is caused by internal resistance and refers to the deviation between $V_{operating}$ and OCV of a battery [37].

$$Overvoltage = OCV - CCV \tag{2.1}$$

As stated in [38], overvoltage serves as an indicator of battery inefficiency. It is expected that the overvoltage will increase as the battery ages or degrades. This is due to the fact that at larger overvoltages the charge/discharge cut-off voltage is reached faster, which is limited by the capacity of the cells. In a study by [37], LFP and NMC batteries were analyzed, and it was found that, in general, overvoltage increases with cycling. Additionally, the overvoltage is greater during charging than during discharging [34]; which indicate that more energy is lost during charging as the battery ages. Moreover, overvoltage is dependent on the C-rate as well as the SOC. High C-rates are linked with higher voltages and, ultimately, an increase in overvoltages. This is demonstrated in [35] where they explore the relationship between OCV vs. SOC and CCV vs. SOC. And conclude that the deviation between OCV and CCV, i.e., overvoltages, is lowest when the C-rate is low, both during charging and discharging. In terms of the relation between the SOC levels and overvoltages, the primary findings of [38] were that when the SOC of a battery is close to full or empty, the electrodes experience greater stress and volume changes, resulting in increased overvoltage. Therefore, limiting the working SOC range is one way to increase battery efficiency, and an overvoltage analysis can provide valuable insight for determining the appropriate SOC range. Additionally, temperature can also have a significant impact; high current rates and low temperatures can result in high overvoltages, leading to lower voltaic efficiency.

2.3.4 Lifetime

The cycle life is an estimation of how many cycles a battery can provide before it reaches its end of life (EOL). The battery is considered EOL when its actual capacity decreases to $60\% - 80\%$ of its nominal capacity at the beginning of life [27]. The shelf life or storage life of a battery refers to the duration for which it can be stored under specific conditions before it expires. This duration is dependent on the battery's chemical composition and design, as well as the operating conditions to which it is subjected [8]. Even when a battery is not in use, it undergoes degeneration processes such as self-discharge, which can affect its performance. There are two types of aging that can occur in a battery: calendar aging, which includes shelf life- or storage life considerations, and cycle aging, which includes cycle life considerations.

2.3.4.1 Cycle Aging

Cycle aging is mainly due to permanent damage in the battery's chemistry during cycling, for example, loss of lithium ions measured through the coulombic efficiency. Deep discharge cycles and overcharging will especially contribute to shortening the cycle life [32]. In addition to this, there is an established correlation between increasing ambient temperatures and the degradation rate of maximum capacity during cycling. This is due to the fact that degradation mechanisms that lead to irreversible capacity loss are accelerated by elevated temperatures. According to [39] both high and low temperatures cause a decrease in cycle life.

2.3.4.2 Self-discharge (Calendar Aging)

The main factors that affect calendar aging are storage time, SOC level, and temperature [8]. Due to chemical processes, the battery will lose capacity when it is not in operation; this degradation process is referred to as self-discharge. Usually, the rate of self-discharge increases with temperature, which is illustrated in [14]. They estimated that the monthly self-discharge of a li-ion battery when stored at 50 % SOC is $\approx$ 0.5 % at $25°C$ and increases to $\approx$ 1% at $45°C$. At a fixed temperature, degradation occurs faster at higher SOC levels, this was verified by [36] and they suggested that avoiding high SOC will increase batteries lifetime. Although previous literature [40] stated that both high and low SOC contribute equally to aging the battery, [36] states that low SOC levels are less detrimental compared to high SOC levels. Another property of self-discharge is that it's not linear with time and is usually higher right after operation; this effect is called the relaxation effect [41]. According to [42], when a Li-ion battery is fully charged, it has twice as much self-discharge in the first 24 hours compared to the rest of the month. The self-discharge is measured through OCV, and using traditional methods, measuring the self-discharge can take up to one month,

alternatively [43] suggests a method to measure the self-discharge of the battery in 24 hours.

2.4 Auxiliary Subsystem

The auxiliary system consists of various subsystems that are usually responsible for managing and controlling the battery and BESS. The main components are the control systems and thermal management systems. The control system plays a critical role in ensuring the proper functioning of BESS and its subsystems. The overall operation of the BESS is usually managed by a supervisory controller, which is responsible for communicating with the external environment. Additionally, the BESS is equipped with an inner management system, such as the BMS, which ensures the safe operation of the battery pack. Finally, the TMS is responsible for regulating the temperature within the BESS to ensure safe and optimal operation.

2.4.1 Supervisory Controller

One type of supervisory controller is the EMS [44]. For a standalone BESS, the EMS acts as the link between grid demand and the BMS and is an overall energy management system that balances multiple generation resources based on grid requirements. For example, in a PV-BESS setup, an EMS can balance the outputs from PV and BESS simultaneously. It dictates when to start charging or discharging the battery based on production scenarios or customer agreements. The EMS can also be programmed to decide whether the BESS should be charged from the PV resource or from the grid.

2.4.2 BMS - Fault Detection

The primary purpose of a BMS is to ensure the safe and reliable operation of batteries through fault detection. The BMS collects essential data such as voltage, current, and temperature and uses that data to prevent the battery from operating outside the safe operating area (SOA) [45]. When the BMS detects unacceptable voltages, it will disconnect the battery cells from the circuit. The SOA is limited by the following regions: the over-temperature region, which can cause thermal runaway; the overcharge region, which can trigger thermal runaway and reduce the overall capacity of the battery cell; the over-discharge region, which can cause electrochemical imbalances and create dendritic growth that can lead to shorts within a cell; and the under-temperature region, which is similar to the over-discharge scenario. The thresholds are determined based on the chemistry and design of the battery. An example of a SOA is illustrated in Figure 2.2.

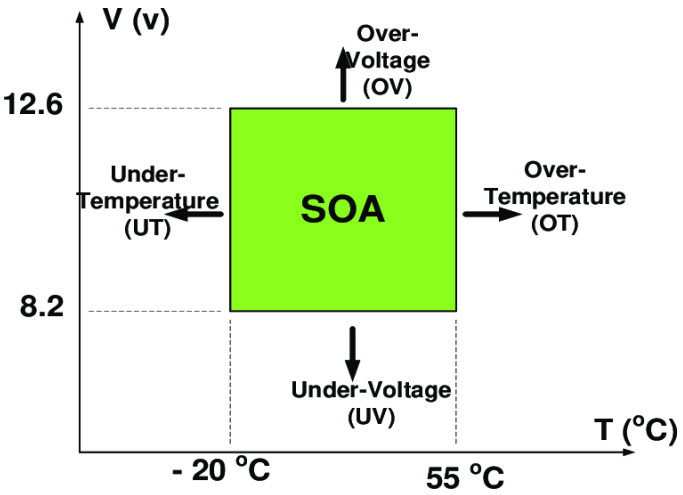

Figure 2.2: SOA for a lithium-polymer battery. (Source: [46])

Additionally, the BMS algorithm can estimate other important battery parameters, such as SOC and state of health (SOH), by utilizing the collected data and relevant models. Tracking these parameters not only helps in prolonging battery life, but also enables better energy utilization [45, 47, 10].

2.4.2.1 State of Charge

The two most common methods for estimating the SOC of the battery are the coulomb counting method and the voltage method. The Coulomb counting method estimates the SOC of a battery by using current measurements. According to [48], the equation is approximately

$$SOC_{t1} = SOC_{t0} - \int_{t0}^{t1} \eta_i \frac{i(\tau)d\tau}{C_{max}}$$

Where η_i is the charging(0.98-1)- or discharging(1) efficiency and can be approximated to 1. This equation is the most common way to estimate the SOC due to its simplicity. However, its accuracy relies on an estimation of the initial point, SOC_{t0}, which is difficult to obtain without external input. Another issue is that it relies on accurate measurements of the current, which are often affected by external factors, such as the measuring equipment. The degradation of the battery capacity can also affect the accuracy of the SOC estimation. On the other hand, the voltage method utilizes the relationship between CCV and SOC. According to [45], the voltage method for SOC estimation is reliable for constant or low loads, such as cellphones with a single cell or for NMC chemistry, but not as much for LFP due to its flat voltage profile. The voltage method becomes less reliable with dynamic, heavy loads or batteries with widely varying temperatures. A third option is a combination of Coulomb counting and the voltage method, which is what is most commonly used today. These two meth-

ods can compensate for each other's shortcomings and provide higher accuracy when combined. There are two ways to combine these: through a weighted method that gives different weights for each SOC estimation, or by primarily using the Coulomb counting method and the voltage method for the initial SOC value to reset the capacity.

In terms of the expected shape of the SOC curve, it will differ depending on how the battery is operated. One simple and commonly used application when illustrating the BESS in PV is load following or increasing self-consumption, which refers to maximizing the self-consumption of the on-site generated power. This strategy is illustrated by [49] in Figure 2.3. Prior to surplus PV production, the SOC remains

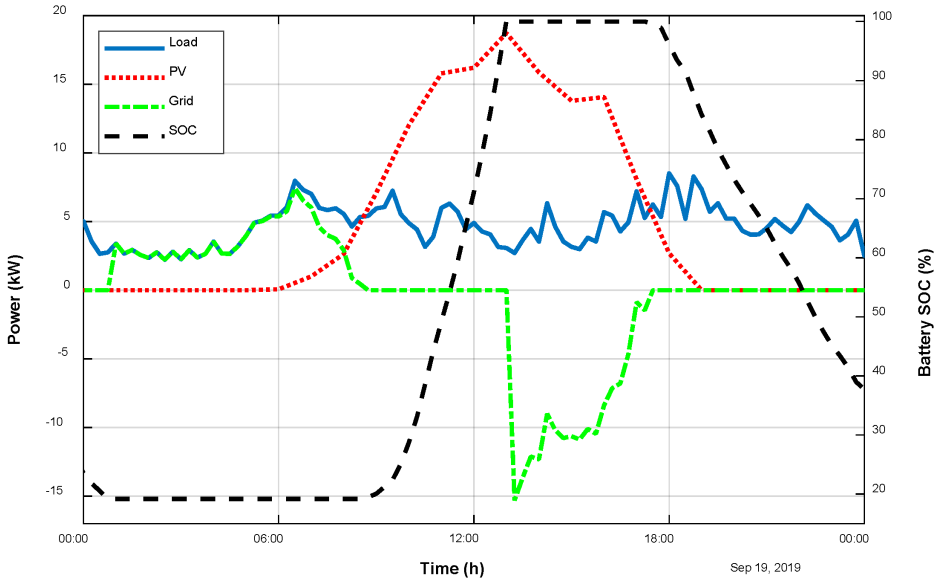

Figure 2.3: The SOC (black) curve for BESS in load following applications is presented along with the power from the grid (green), PV (red), and load (blue) at each hour. (Source: [49])

constant, indicating that the BESS system is on standby. The SOC begins to rise around noon when PV generation surpasses the load, resulting in excess energy generation. The increase in SOC implies that the BESS is charging, and it continues to do so until it reaches its full capacity, indicated by an SOC of 100%. Any surplus PV production beyond this point is then exported to the grid. Conversely, when the PV generation falls below the load, the SOC begins to decrease, indicating that the BESS is discharging, and the load is now powered by the BESS instead of the grid. During the charging process, it is expected that the SOC will rise linearly, indicating a constant C-rate. However, during the discharging phase, slight deviations in the slope may occur due to variations in load and supply. Additionally, it is noted that the SOC starts at 20%, not 0%. This is due to the negative effects of low SOC levels on energy and capacity losses.

2.4.2.2 State of Health

The BMS is also responsible for measuring the SOH of the battery. SOH is the measurement of the capacity decrease of the battery and is used to determine the EOL of the battery. It can also be used to track the health of the battery under different conditions to determine optimal parameters and environments, as well as for various cost analyses. The SOH of batteries is usually defined from the perspectives of capacity loss and impedance increase [50]. The easiest method of tracking SOH is through the capacity loss, which requires monitoring maximum discharged capacity over time. The other method is through cell impedance, this is because it increases with each cycle and can therefore be used to assess the cycle life of a battery. However, impedance is also affected by other mechanisms, such as cell leakage if internal or external connections in battery packs are broken or temperature [45].

2.4.3 Thermal Management System

Important metrics in this section are operating temperature, recommended temperature, and storage temperature. The operating temperature refers to the allowed temperature range of the immediate local environment at which the battery can operate. The recommended operating temperature is usually lower than the storage temperature, and the storage temperature is the temperature range that the immediate surrounding environment of the battery should be kept at when storing the battery.

2.4.3.1 Temperature Effects on BESS

According to [39], the Arrhenius equation shows that at higher temperatures, the battery's power output increases. The heat output of the battery is second-order proportional to the discharged current, which can be represented as

$$Q_{res} = I^2 R$$

Where Q_{res} is the generated heat, I is the current and R is the internal resistance. The proportionality between heat and resistance means that both increased internal resistance and current produce heat, but also that increased ambient temperatures provide an increase in internal resistance. Low temperatures also affect battery performance. The study [14] discusses how charge and discharge resistances increase with an extreme decrease in temperature due to the slow-down of electrochemical and physical processes. Furthermore, storing the battery at higher temperatures results in higher self-discharge, and both the cycle life and shelf life of the battery are dependent on temperature. Thus, increased temperature will have a significant impact on the degradation rate of the battery's lifetime. In a particular setting, [51] estimated that the

degradation rate of the actual capacity of a lithium cobalt oxide battery will become twice as high for the first 200 cycles when the temperature is increased from 25°C to 45°C.

The impact of temperature on batteries can be divided into internal and external impacts. Internal impact refers to heat generated due to internal resistance, which is reflected as power loss in the circuit. External impact of temperature refers to the effect of the surrounding environment on the battery, such as too hot or too cold climates with temperatures outside the operational temperature. If the battery voltage exceeds the maximum voltage of the battery due to overcharging or over-discharging, high C-rates will also cause increased internal resistance [39]. Increased internal resistance is linked with energy loss and will generate heat, which, when high enough, causes thermal runaway. Thermal runaway is when the battery overheats uncontrollably, ignites a fire, and, in the worst case scenario, causes an explosion [27]. Usually, the BMS will disconnect the battery from the circuit when the voltage falls outside a safety threshold to ensure safe operation. Therefore, to make sure the BESS doesn't disconnect during operation, the temperature needs to fall within the operating temperature range.

2.4.3.2 Thermal Management Systems

A thermal management system (TMS) is used to maintain the temperature within the operating temperature range. TMS accounts for both cooling and heating. However, it is usually designed to cool down the system when the battery pack heats up due to internal heat generation during operation. The most common method for thermal management is natural convection or air cooling.

In the literature, there are passive and active cooling methods. Passive cooling utilizes designs that allow for natural convection or phase-change materials and doesn't consume external energy. For low discharged power, it is possible to utilize natural convection. However, when the power output increases, active cooling is necessary [39]. Active cooling applies external force to remove heat. Among active cooling methods, there are air cooling and liquid cooling. Air cooling refers to allowing colder air flow into the system through air fans or air conditions. Air cooling is the preferred TMS due to its simple design and its ability to evenly distribute heat dissipation at a low cost. Liquid cooling uses liquids with certain properties to absorb heat from the environment and transport it out of the system. Direct liquid cooling is when the liquid is in direct contact with the battery and has the ability to flow between battery packs, similar to air. Indirect liquid cooling requires a cooling block that is placed beside the battery pack. The comparative study, [52] compares natural convection, air cooling, and liquid cooling and concludes that the use of natural convection alone is limited in

protecting the battery from high temperatures. Air cooling showed better results at managing the temperature, and direct cooling was most efficient at cooling the battery pack. Similarly, [53] compares direct air and liquid cooling methods to regulate temperature increases. The results showed that while air cooling is limited for higher heat loads due to its heat transfer capability, liquid cooling can remove higher heat loads. The disadvantage of liquid cooling is that it is often more expensive, complex, and susceptible to malfunction.

2.4.4 Auxiliary System - Power Consumption

The study, conducted by [22], investigated the power consumption demand of auxiliary systems in BESS. Through simulations of BESS in frequency regulation applications, they found that high temperatures required maximum auxiliary power, medium ambient temperatures required the minimum auxiliary power, and for lower temperatures than that, the power demand rose again. In their analyses, they looked at the effect of power input vs. RTE of BESS. They found that lower power input put more weight on the losses due to auxiliary system demand, and that these losses had less impact when the input was higher. The main influencing factor for higher system consumption is higher power input. Additionally, similar to the battery, the type of technology used for TMS and supervisory controller is also a determining factor for the final system consumption.

2.5 Loss Mechanisms Overview

The following table provides an overview of the loss mechanisms identified in this review associated with BESS efficiency. From left to right, the table starts by listing each subsystem in the BESS, followed by a list of typical components included in the subsystem. For each subsystem, a summary of loss mechanisms that typically occur during operation is listed, and finally, the influencing factors for each loss mechanism are listed, which refer to the factors that trigger or impact them. Among the influencing factors in Table 2.2, there are several that are possible to measure and others that are out of scope for the following analysis. Most specifically, the power input, C-rate, SOC range, and idle period are metrics possible to extract from operational data and will be used for the analysis in Chapter 4. As discussed in Section 2.4.2 the BMS doesn't directly measure metrics such as SOC but uses models such as Coulomb counting and the voltage method, which each have their weaknesses, something worth considering when conducting analysis.

Subsystem	Components	Loss Mechanisms	Influencing factors
PE	Rectifier	Switching	Switch Count, T
	Inverter	Conducting	Power Input, T
		No-load current	Idle Period
Battery	Battery cells	Overvoltage	Age, C-rate
			SOC range, T,
			Technology
		Internal Resistance	C-rate, Power input
			SOC level, T,
			Technology
Auxiliary	BMS/EMS	Power Consumption	Design, Capacity
	TMS	Power Consumption	Design, Ambient T

Table 2.2: An overview of the loss mechanisms found in each subsystem of BESS and the related influencing factors.

Methodology

This chapter explains the various strategies and models utilized for calculating RTE and the actual capacity of a BESS under operation. The chapter begins by describing the BESS system and the relevant application applied. Subsequently, the system boundaries for the calculations are defined, and a system sketch is presented, highlighting relevant categories within the system. Prior to explaining the calculations, the data cleaning and handling approach is described. Then, the RTE calculations are presented, along with an approach termed the 'detailed component efficiency analysis', battery efficiency, voltaic efficiency, and coulombic efficiency. The approach used for evaluating the RTE computations will be presented, as will the approach to investigating the impact of operational parameters on system efficiency. Finally, the two approaches for calculating actual capacity are presented, one utilizing a manual approach to find the maximum DOD and the other utilizing rainflow counting. The results for these calculations are presented in Appendix 2.

Figure 3.1: Pictures of the installation of BESS and PV on a farmhouse in Bjorkelangen. Source: Solcellespesialisten AS

3.1 Data Site and System Spesifications

The BESS system under consideration is located in Bjorkelangen, Norway, and the data used in this study was recorded during the period of April 2022. The weather

during this period exhibited temperatures within the range of [0,8]$°C$, along with some periods of wind and rain. This is relevant since the weather conditions have an indirect impact on the SOC curve for this BESS application due to the fact that the energy yield of the PV system is influenced by the weather conditions. Figure 3.1 depicts images of the installation of the BESS and PV system.

3.1.1 Battery System Specifications

There are two ways to incorporate BESS into PV-grid systems: AC-coupled and DC-coupled [11]. Although the DC-coupled option is more versatile in its suitability for different applications and does have a higher PV-to-grid and PV-to-battery efficiency than the AC-coupled BESS, the entire system is dependent on one inverter, so in the event of a malfunction, the entire system will be affected, and both BESS and PV will be limited by inverter capacity. In AC-coupled systems, there are two inverters, one for the BESS and another for the PV system. With this system configuration, the power to the grid can be maximized by discharging both the BESS and PV at their maximum power. The BESS utilized for this research is an AC-coupled system, meaning that it

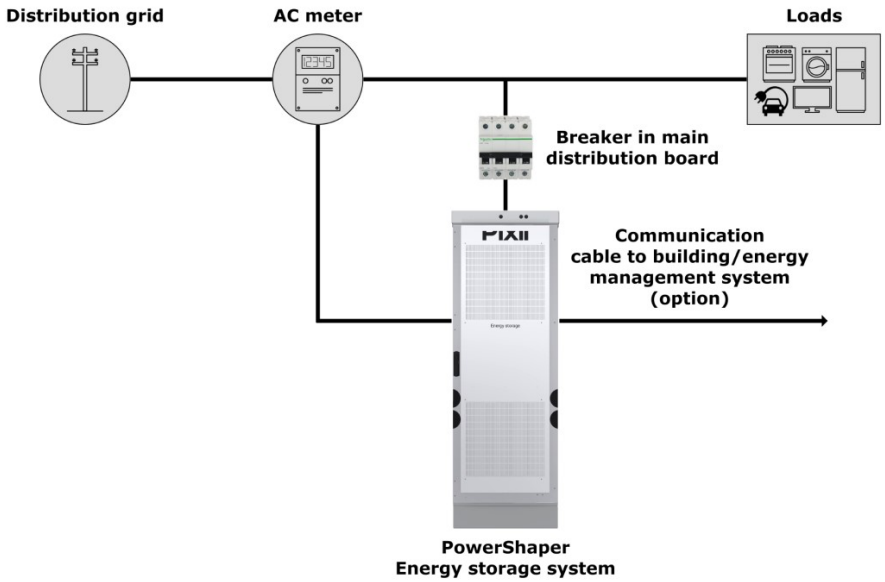

Figure 3.2: Behind-the-meter application, picture taken from the Pixii installation guide for PowerShaper Source: Pixii AS

is directly connected to the AC grid. This is illustrated in Figure 3.2, which depicts a diagram outlining the incorporation of the module into the system. The BESS module is provided by PIXII and is a comprehensive system that includes power electronics and other necessary subsystems. The battery subsystem in this study consists of three NMC batteries, specifically the 'LG Chem 48V Standalone Battery Module', which are connected in parallel. The specifications for these batteries are presented in Table 3.1,

which is also found in the catalog provided by the manufacturer. The cooling system in this setup is passive air cooling, which is utilized for both the battery and converter systems. The air is filtered before it is utilized for cooling purposes. The temperature sensors used for measuring the temperature are positioned inside the battery system, between the battery cells.

Parameter	Value
Nominal Charge Capacity	3x126Ah
Nominal Energy Capacity	3x6.52 kWh
V_{Nom}	51.8V
$V_{Operating}$	42-58.8V
Max. Charge/Discharge Current	3x63A
Max. Charge/Discharge Power	3.26kW
Round trip efficiency	95% or more
Cooling Type	Forced Air cooling/Natural convection
Available Operating Temperature	-10 45°C
Optimal operating Temperature	15-30°C
Storage Temperature	-30-60°C
Self-Discharge Rate During Storage,	Less than 6% per year at 25°C
Humidity	$5\% - 95\%$
Altitude	Below 2,000m

Table 3.1: Battery specs for three LG Chem 48V stand-alone battery modules. Source: LGChem

3.1.2 Strategy of The Battery System

The strategy implemented in this system was aimed at smoothing out energy prices, also referred to as PS. The objective was to increase self-consumption during expensive hours. The EMS was programmed to execute a simple application by charging the battery during high PV production and low electricity prices and discharging the battery during low PV production and high electricity prices. In practice, the BESS was set to charge and discharge at times when the prices were expected to be low and high, respectively, based on patterns in the electricity market. The BMS restricted the SOC at the lower limit of 15% and the upper limit of 90%, however, the management systems did not place a lower limit for power input. For the SOC calculations, the BMS used a combination of coulomb counting and the voltage method. If there was no production for an extended period and there was a chance that the SOC fell below 15% due to losses on standby, the BESS would be charged by the grid, enough to maintain the required SOC level. The SOC of the battery was regularly re-calibrated during maintenance to accommodate potential capacity fade. Figure 3.3 illustrates the estimated SOC curve for this type of application on this BESS.

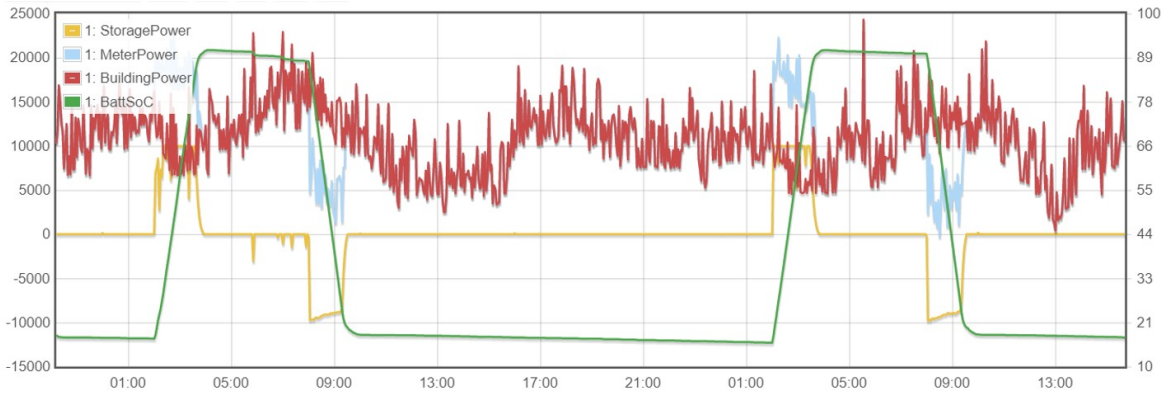

Figure 3.3: The P_{BESS} (yellow), meter (blue), and building (red) along with the SOC curve (green) Source: Solcellespesialisten AS

3.2 System Boundaries

The dataset under consideration represents a complex system with three primary components: "meter,' which records the power to the grid; "building,' which is the net power between the PV component and electric energy consumption component; and 'BESS,' which has been previously described. Figure 3.4 presents an illustration of this system based on the available data, with the dotted line indicating the BESS. Within the BESS, two subsystems will be examined: the "power conversion subsystem,' which refers to power electronics such as converters for AC-DC conversion and vice versa; and the "battery,' which refers to a pack of batteries that are connected in parallel. The auxiliary system depicted in the sketch is not a gathered entity; in reality, the fans, and heaters are located both between the electronics and the battery pack as well as on the outside of these components. The entire system operates without external power consumption. Only the battery and power electronics will be evaluated explicitly, due to the limited information in the data concerning the auxiliary system.

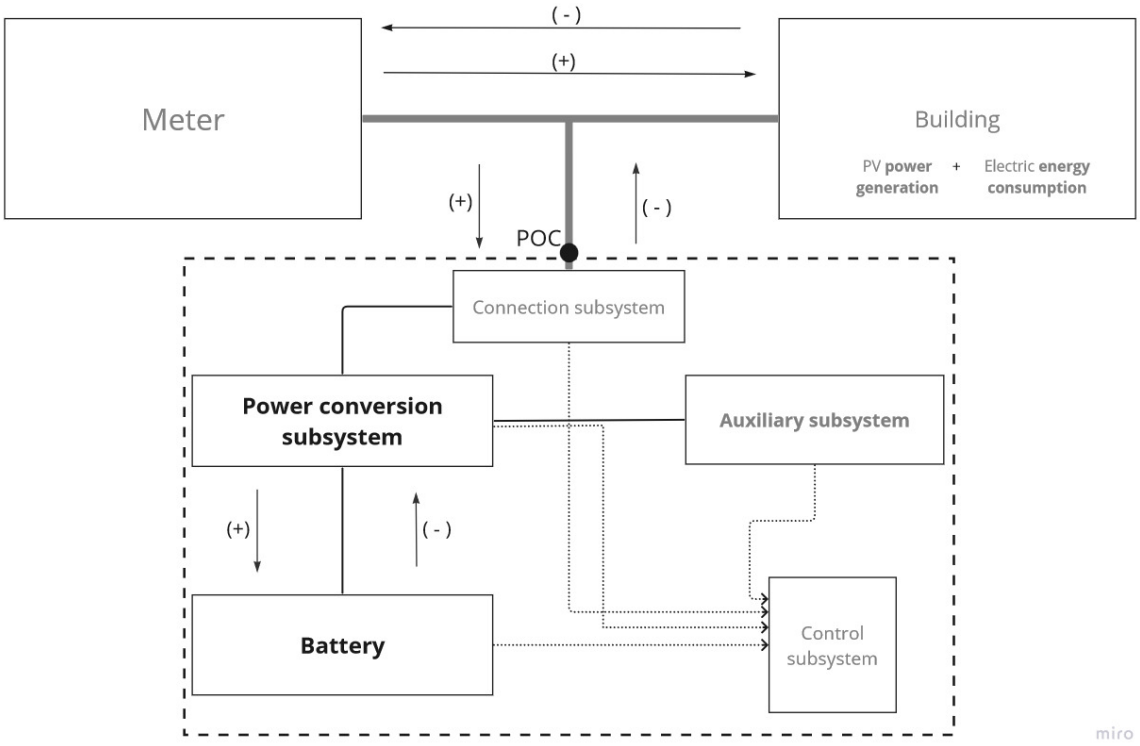

Figure 3.4: A schematic representation of the BESS based on the information gathered from the available data, the gray parts are considered to be outside the scope of the analysis. The arrows in the figure indicate the directions of flow and their corresponding signs.

3.3 Cleaning and Preparing The Data

This section describes the initial data handling process, including the examination of scattered values and missing data. The dataset was inspected to ensure that it contained only reasonable values. The first dataset, Set1, included measurements of timestamp, power at BESS (P_{BESS}), and SOC and covers the time period between April 1 and April 30, 2022, providing measurements at minute-level resolution. The second dataset, Set2, additionally included BMS data such as battery voltage, battery current, and maximum temperature, with the data being presented as aggregated hourly data.

According to the IEC standard [13], the recommended sample time for BMS data such as SOC, temperature, and voltage is $\leq$ 1 minute. The recommended sample time for data measured at POC is dependent on the BESS system application. The available BMS data is provided in aggregated hourly format, which is an important consideration when discussing the results. The data measured at POC is available in minute-level format, and an overview of the data can be seen in Table 3.2.

Data	Set1	Set2
Time period	1-30. April 2022	4-15. April 2022
Columns	Timestamp P_{BESS} SOC	Timestamp P_{BESS} SOC, Voltage Current, Max.T
Sample time	1 min	1 hour

Table 3.2: Properties of two datasets available for analysis. Set1, which provides measurements in 1 minute intervals, and Set2, which provides measurements in 1 hour intervals.

3.3.1 Scattered Values and Missing Data

Before doing any analysis with measured data, the quality of the data had to be assessed. It was important to make sure that the data points were organized within their respective columns and that the value for each entry was reasonable. Any columns that didn't contain valuable information were removed; for example, random scattered values created unnamed columns. For Set2, this was sufficient in terms of data cleaning. However, for Set1 the cleaning process continued. In the case that a non-float value was found in a column that was supposed to contain float values, it was converted to a "Not a Number" (NaN). This was done on both P_{BESS} and SOC. Any values under timestamp that were not in timestamp format were also converted to NaN. At this point, the columns contained a significant number of NaN values. There are different strategies for handling NaN; for a description and overview of all strategies, see [54]. Since both SOC and power were important for calculations, deciding to delete NaN values meant that the entire row where the NaN value was located would also be eliminated, which would result in losing valuable information and was therefore avoided. The other option was to replace the NaN value with a representative. In that case, the shape of the curve was the important property to preserve, and interpolation was used to estimate the shape of the curve between two points. There are three different interpolation methods: polynomial, linear, and quadratic. Since the sample time is 1 minute and for this application it is not expected that the frequency is high, linear interpolation was applied.

It was not sufficient to eliminate NaN values; the data also had to be reasonable. The values needed to fall within the possible realm. For example, SOC couldn't have negative values, and the P_{BESS} couldn't go beyond its maximum or minimum values. Luckily, all the values made sense from a physical point of view. In addition to this, it was expected that there would be 1440 minutes per day. Most days did not satisfy this expectation and had minute gaps scattered all over the column. For this analysis, the length of each period had to match. Since the missing values usually occurred

outside the operational period while the BESS was in standby, the SOC and power had a linear trend. Therefore, the mean value between two points was expected to be representative of the middle value. By using a timestamp and locating where the time skipped, the mean values of the two points were inserted between them; see Table 3.3 for further illustration. This strategy only fills gaps where the timestamp skipped one

Time [hh:mm:ss]	SOC	PowerShaper
00:06:30	18.1	0.00
	(insert mean values here)	
00:08:30	18.1	0.00

Table 3.3: Illustration of inserting mean values for skipping small intervals of data.

minute. Any larger gaps that were avoided. After inserting mean values as explained, full days now have 1440 or 1339 data points; any data points less than that were classified as incomplete days and will be discussed under results.

3.3.2 Separating The Data

The raw data did not distinguish between charging and discharging. It was therefore important to 'separate' the data to get curves that represented charging and discharging separately. The decision of which sign to use for which operation was determined through the SOC. If the SOC increased, it meant that the energy was charged into the battery, and if it decreased, it meant that the energy was discharged out of the battery. Based on this, the definitions of 'charging' and 'discharging' in the BESS were decided. For P_{BESS}, when it was negative, the BESS was discharging, when positive, it was charging, and when 0 it was on standby. Here, "standby" doesn't refer to the battery being in standby mode; rather, it refers to the BESS not being in operation.

The following list represents a simple pseudocode to explain the algorithm for the function used to separate the curve into each state.

- **Input**: Set1 (State, P_{BESS}) or Set2 (State, P_{BESS}, $P_{Battery}$)
- For each state:
  - Create a data frame
  - Append input parameters relevant to the state
  - Set non-relevant values to zero
- **Return**: Set1-charge, Set1-discharge, Set1-standby or Set2-charge, Set2-discharge, Set2-standby.

The function takes as input a data frame with columns for 'state' and 'power'. The 'state' column can have one of three possible string values: "charging, "discharging, and "standby." The function creates a new data frame for each state and appends the relevant value for each parameter to it. Any values that do not correspond to the required state are set to zero. The function then returns three data frames: one for when the BESS is charging, one for when it is discharging, and one for when it is in standby mode.

3.3.3 Numerical Integration

The accuracy of energy calculations is a crucial factor in the accuracy of RTE calculations. In this research, the energy is determined by numerically integrating the power curve over the desired time interval. While there are several approaches to numerical integration, the most commonly used methods due to their simplicity are Simpson's and the trapezoidal rule. The Trapezoidal rule approximates the definite integral by using a trapezoidal shape to approximate the area under the input curve. In contrast, Simpson's rule utilizes parabolas to approximate the same curve. A comparison analysis of the accuracy of these two methods conducted by [55, 56] concluded that both methods are fairly accurate compared to other simple methods, but Simpson's rule is slightly more accurate than the Trapezoidal rule. Therefore, for this research, Simpson's rule will be used for numerical integration. The numerical integration methods will be imported from the scipy.integrate library in Python and applied to the calculations. For a more detailed explanation of the functionality and properties of Simpson's rule, see [55].

3.4 Round Trip Efficiency

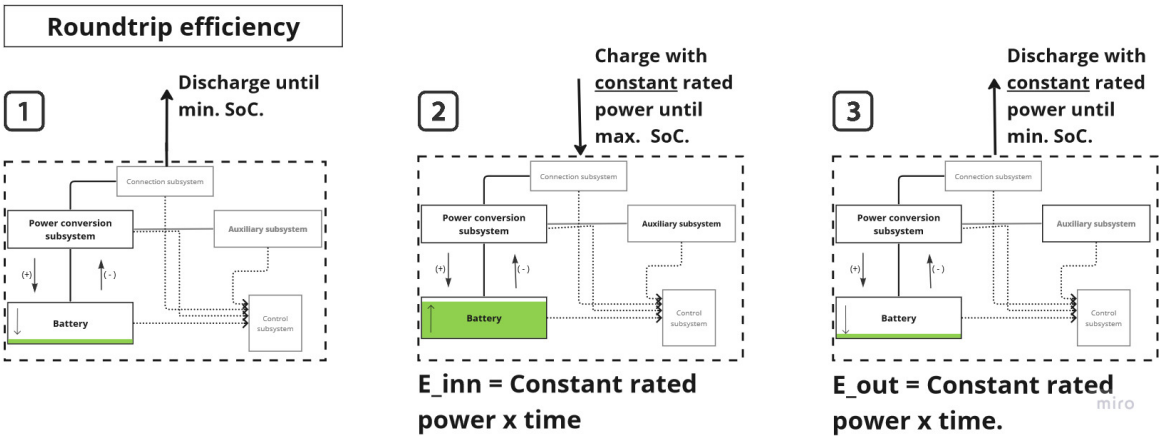

Figure 3.5: An illustration of the steps for measuring and calculating the BESSs RTE according to [13].

According to the duty cycle energy efficiency test specified in the IEC standard [13], it is recommended to charge and discharge the BESS using a constant rated power during a specified time period where the initial and final SOC values are the same. Figure 3.5 illustrates the step-by-step process outlined in the standard, which allows for the energy calculation without the use of numerical integration. This is due to the fact that when the power remains constant, the area under the curve is equivalent to that of a rectangle, which is simply the product of the x-axis and the y-axis.

Since it is difficult to maintain constant power and standard conditions in operational settings, the main condition will be that the energy input is matched with the energy output from the BESS such that the initial and end values for the SOC are the same. Any deviation in the discharged energy reflects internal energy losses. Energy input and output are calculated from the power curve P_{BESS} over a desired time period Δt, which is then numerically integrated using Simpson's rule to obtain the energy ε_{BESS}.

$$E_{BESS} = \int_{t0}^{t1} p_{BESS}(\tau)\ d\tau$$

Finally, the RTE is found through the ratio between energy discharged $E_{BESS-out}$ and energy charged $E_{BESS-in}$.

$$\varepsilon_{BESS} = \frac{E_{BESS-out}}{E_{BESS-in}}$$

3.4.1 Detailed Component Efficiency Analysis

A detailed component analysis provides insight into the internal losses of a BESS. The main concept is breaking down the losses into five steps to allow for the identification of the specific areas where energy losses occur. This approach is based on the methodology described in [14], which maps out a total of 18 loss mechanisms to use in their analysis. The detailed component efficiency analysis involves calculating five efficiencies, which represent the efficiencies at five specified locations within the BESS. This approach is illustrated in Figure 3.6. The efficiencies are obtained by finding the ratio of energy output at each step compared to the initial energy input.

Step	1	2	3	4	5
Efficiency[%]	1.0	2.0	3.0	4.0	5.0

Table 3.4: An example of the results from the detailed component analysis. It contains five efficiencies, representing the efficiency for each step illustrated in Figure 3.6.

Table 3.4 shows an example of how the result can look, where the integers 1.0 to 5.0 represent the calculated efficiency at each step. Step one is the energy input into

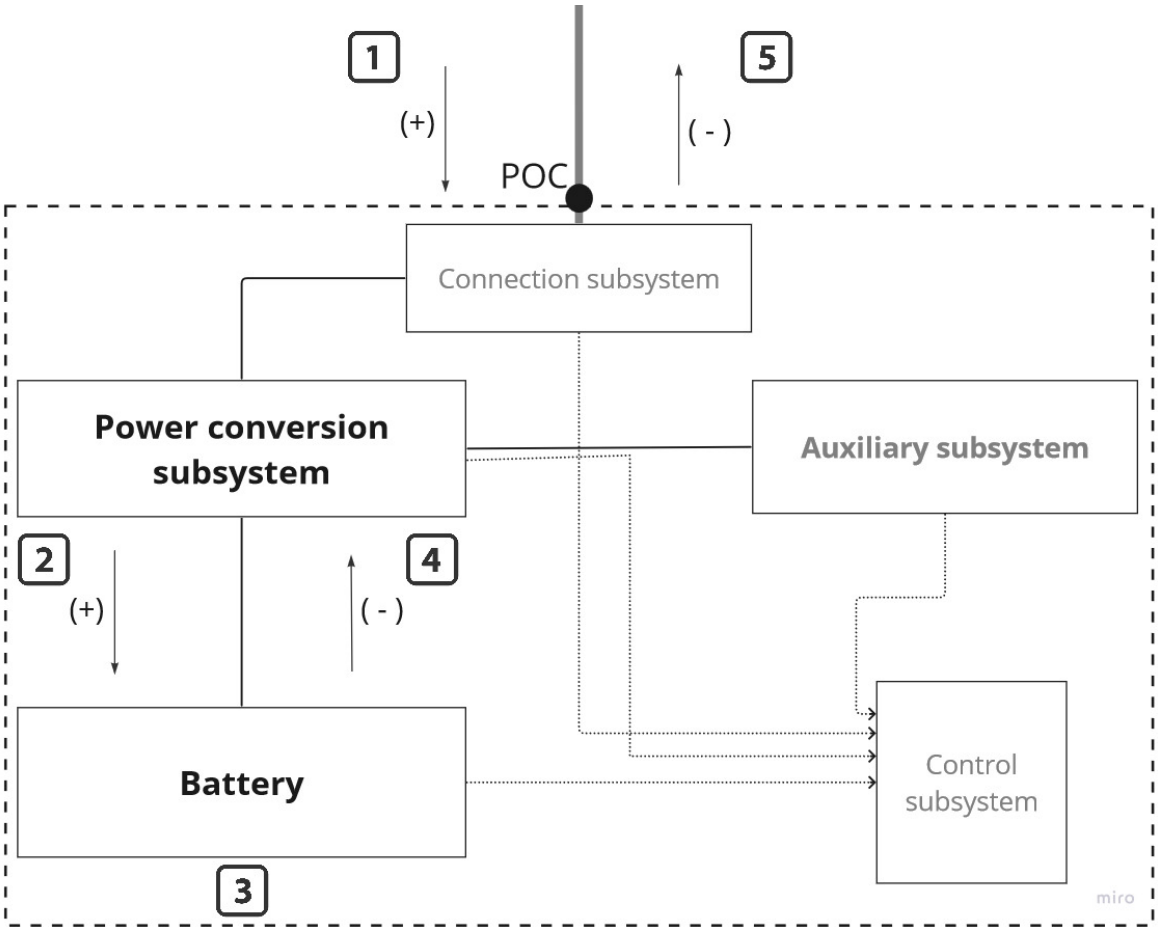

Figure 3.6: Diagram that illustrates where each step in the detailed component analysis is located.

the battery system; this will act as the reference point for all the calculations, and the efficiency at this point will be 100%. Step two is the AC to DC conversion; the efficiency at this point will reflect the losses tied to the AC to DC conversion process. Step three reflects how much power loss there is in the system when the BESS is in standby; this is also compared to the reference at point 1. Step four is the power that is discharged from the battery before DC-AC conversion, and step five is the power out of the system after the final conversion and represents the total losses of the BESS. To relate losses to each component. Table 3.5 illustrates the calculations to find the energy losses.

The total conversion losses are the difference between points 1 and 5. The losses tied to the first conversion are the difference between points 1 and 2 and are named 'rectifier'. The losses due to the final conversion are the difference between points 4 and 5 and are called "inverter". The difference between point 4 and point 2 is used to find the total losses in the battery, and point 3 indicates the losses in the battery when BESS is in standby. The remaining losses are categorized as "other" and refer

BESS Efficiency	5.0
Conversion Losses[%]	1.0-5.0
Power Conversion[%]	(1.0-2.0)+(4.0-5.0)
Rectifier[%]	1.0-2.0
Inverter[%]	4.0-5.0
Battery[%]	2.0-4.0
Standby[%]	3.0
Other[%]	(2.0-4.0)-3.0

Table 3.5: A sample of calculations to find the energy losses in % relative to input for each step, illustrated in Figure 3.6 by using results in Table 3.4.

to losses in the battery during operation.

The function used for the detailed component efficiency analysis is explained by the following list, which represents a simple pseudocode.

> **Input**: Set2(State, P_{BESS},$P_{Battery}$)

> Apply function to separate the curves. Which returns: Set2-charge, Set2-discharge, Set2-standby

> Apply numerical integration on each state for P_{BESS},$P_{Battery}$ to find the energy

> Calculate efficiencies

» Step 1: $\frac{P_{BESS_{Charge}}}{P_{BESS_{Charge}}}$

» Step 2: $\frac{P_{Battery_{Charge}}}{P_{BESS_{Charge}}}$

» Step 3: $\frac{P_{Battery_{Standby}}}{P_{BESS_{Charge}}}$

» Step 4: $\frac{P_{Battery_{Discharge}}}{P_{BESS_{Charge}}}$

» Step 5: $\frac{P_{BESS_{Discharge}}}{P_{BESS_{Charge}}}$

> **Return**: 5 efficiencies.

The function takes as input a data frame containing the states P_{BESS} and $P_{Battery}$. First, the split function as described in Section 3.3.2 is applied to split the input curves into charging, discharging, and standby. Next, numerical integration is used to calculate the energy in each state. Finally, the five efficiencies are calculated using the methodology outlined for the detailed component analysis. The function returns five efficiency values.

3.4.2 Battery Efficiency

The data from the BMS also enables the determination of the battery's RTE. There are three efficiency metrics relevant to the battery, namely energy efficiency ($\eta_{E_{Bat}}$), coulombic efficiency (η_C), and voltaic efficiency (η_V). To perform the necessary calculations, the data was separated with the split function outlined in Section 3.3.2.

3.4.2.1 Energy Efficiency

The energy of the battery $\varepsilon_{Battery}$ is the area under the $P_{Battery}$ or the integration of $P_{Battery}$ over a time Δt.

$$\varepsilon_{Bat} = \int_{t0}^{t1} p_{Bat}(\tau)\ d\tau$$

And $\eta_{E_{Bat}}$ is the ratio between the discharged energy ε_{out} and the charged energy ε_{in}.

$$\eta_{E_{Bat}} = \frac{\varepsilon_{Bat-out}}{\varepsilon_{Bat-inn}}$$

3.4.2.2 Coulombic Efficiency

The Coulombic efficiency was found through the ratio between charges. To find the charge, the current curve, I, was integrated over a time, Δt.

$$C = \int_{t0}^{t1} I(\tau)\ d\tau$$

The Coulombic efficiency is the ratio of the charge level when discharged, C_{out}, to the charge level when the battery is charged, C_{inn}.

$$\eta_C = \frac{C_{out}}{C_{inn}}$$

3.4.2.3 Voltaic Efficiency

To find η_V, the ratio between the average voltage of the battery when it's discharged, $\overline{V_{out}}$, versus the average voltage of the battery when it's charged, $\overline{V_{in}}$, was used.

$$\eta_V = \frac{\overline{V_{out}}}{\overline{V_{inn}}}$$

3.5 Parameters Affecting System Efficiency Calculations

3.5.1 "State of Charge" -Correction

According to the standard outlined in [13], the initial SOC and final SOC must be matched. Selecting two matching points in the SOC curve for integration through operational data is not a straightforward process. According to [33], when the integration period is long enough, the impact of varying SOC on efficiency can be minimized. This is because when there is a difference in SOC, the calculated efficiency will not only reflect the actual losses, but also include the energy associated with the SOC difference between t_0 and t_1. Since this analysis seeks to apply efficiency calculations to a shorter time period and, in some instances, there may be a notable difference between the initial and final SOC, the SOC difference cannot be regarded as insignificant. Therefore, the following three suggestions were proposed to correct the SOC difference and reduce it to a level below a specified threshold.

3.5.1.1 Method 1: Using Nominal Capacity

The simplest approach to correcting for the SOC difference is to determine the energy difference associated with the SOC using the nominal capacity of the battery. The nominal capacity of the battery pack used in this analysis is 19.56 kWh. Assuming a linear relationship between SOC and nominal capacity, the SOC_{diff} can be calculated as follows:

$$19.56kWh \times \frac{SOC_{diff}}{100} = E_{SOC_{diff}}$$

And the corrected estimation of the actual efficiency without SOC difference becomes

$$\varepsilon_{corr} = \frac{E_{BESS-out} + E_{SOC_{diff}}}{E_{BESS-in}}$$

3.5.1.2 Method 2: Assumptions Based on Data

This method involves identifying the energy difference based on trends observed in the original data. It can be observed that there is a 0.1% decrease in SOC per hour with a discharge current of -0.5 A. To account for SOC_{diff}, the battery has to "discharge" for $SOC_{diff} \times 10$ hours with a discharge current of -0.5 A. This information can be

utilized to determine the corresponding energy for a positive SOC difference.

$$SOC_{diff} = 0.1\% \times (SOC_{diff} \times 10)$$
$$C_{SOC_{diff}} = -0.5A \times (SOC_{diff} \times 10)h$$
$$E_{SOC_{diff}} = I_{SOC_{diff}} \times 50V$$

And the corrected estimation of the actual efficiency without SOC difference becomes

$$\varepsilon_{corr} = \frac{E_{BESS-out} + E_{SOC_{diff}}}{E_{BESS-in}}$$

3.5.1.3 Method 3

Instead of making any assumptions, this method involves identifying a subset of relevant data where the two endpoints have a minimal SOC difference, while also ensuring that the time period is not reduced more than necessary. This is done to preserve operational conditions as much as possible. An algorithm was utilized to determine the closest point at which the SOC at each end is the same, with a marginal error of $\pm 1\%$. The algorithm is described below:

> **Input**: SOC, P_{BESS}

> Check $Sd = SOC_{t1} - SOC_{t0}$

> If Sd is < 1 then compute ε_{BESS}

> Elif Sd >1 then do the SOC correction:

» Bottom correction: Find the first index where SOC is equal to SOC_{t1}

» Top correction: Find the last index where SOC is equal to SOC_{t0}

» If length of $Bottom_{corr} >$ length of Top_{corr}:

»» Create new dataset with indexes $Bottom_{corr} : SOC_{t1}$

»» Compute ε_{BESS}

» Else:

»» Create new dataset with indexes $SOC_{t0} : Top_{corr}$

»» Compute ε_{BESS}

> **Return**: Dataset for time period where $SOC_{t0} \approx SOCt1$

3.5.2 Temporal Resolution

The data was aggregated into different time intervals to obtain different temporal resolutions. This was done by using minute data to identify representative values for each required interval. For example, for a 20-minute resolution, the mean value for each parameter was calculated for each 20-minute interval to represent that specific time period. As a result, 60 data points for each parameter in each hour were reduced to three representative data points.

3.6 Impact of Operational Parameters on System Efficiency

3.6.1 Calculation of P-rate

The P-rate is a similar concept to the C-rate, and it describes the power rates of the system. While the C-rate provides a direct representation of the charging rate, the P-rate has other influencing factors, such as voltage variations. The relationship between P-rates and C-rates is discussed in [57], where it is noted that the P-rate is typically used in system analysis, while the C-rate is more commonly used in analyses that are sensitive to inaccuracies, such as the assessment of battery cell degradation.

The P-rate is calculated as the power at a specific point in time divided by the battery's capacity. In this study, since the actual capacity of the battery was not available, the nominal capacity specified in the battery pack's data sheet was utilized instead. The resulting P-rate of the BESS was then determined based on the power measurements taken during the system's operation. The P-rate of the BESS was calculated using the formula:

$$P_{Rate} = \frac{P_{BESS}}{19.56kWh}$$

The data contained up to 1440 P-rates per day, and therefore it was impractical to use all of them for a comparative analysis. It was necessary to use a representative value for each day, and since a significant portion of the day is spent in standby mode, during which the P-rate is zero, using the mean value would not be a suitable representation. That's why the maximum P-rate for each day was utilized as a representative value.

3.6.2 Idle Period

The idle period refers to the time period the BESS spent in standby mode. To calculate this, the number of data points for $P_{BESS_{Standby}}$ for each day was used. Since Set1 was

used, the obtained value was divided by 60 to represent the idle period of i hours.

3.7 Methodology - Actual Capacity of a Battery System

In a performance test, the actual capacity of a BESS is defined as the maximum amount of energy that can be discharged at the POC under standard conditions while maintaining a constant rated power output. However, operational data may not always satisfy these criteria. Therefore, in this analysis, the maximum possible discharged energy identified in operational data will be used. For identifying the maximum DOD, two methods are suggested: the first will find DOD by looping through the data, while the second method uses rainflow counting. The results of this analysis are presented in Appendix 1.

3.7.1 Finding DOD - Method 1

This function performed a manual identification of the desired DOD. A simple pseudocode is used to demonstrate the algorithm used to find the actual capacity:

> **Input**: SOC, P_{BESS}

> Locate index where SOC == 18%

> Locate index where SOC == 90%

> If index SOC = 90% < SOC = 18%

» Calculate the energy for relevant interval

> **Return**: Actual capacity

The required data is SOC and P_{BESS}. The function locates the indexes where SOC is approximately 90% and 15%. If the index corresponding to SOC 90% is less than the index corresponding to SOC 15%, then the function uses these indexes to locate the corresponding power curve. The energy is then calculated by performing numerical integration over the relevant time period.

3.7.2 Finding DOD - Method 2 (Rainflow Counting)

Rainflow counting is a commonly used method for cycle identification in various applications. It proposes a method to derive cycles from a given curve based on its properties. In particular, the rainflow algorithm has been shown in several studies to

be useful for extracting certain DOD values from SOC curves and correlating them with energy values in power curves [58, 59, 60]. The rainflow counting algorithm identifies full cycles, which involve a full cycle of charging and discharging, as well as half cycles, which involve only one of these processes. It is possible to understand the specifications and methodology in detail in [58, 59, 60].

The algorithm used for finding the actual capacity through rainflow counting is described below:

- **Input**: State, SOC, P_{BESS}
- Apply rainflow counting to SOC
  - Output: DOD, index-start, index-end
- Identify relevant DOD and use the indexes to calculate the energy.
- **Return**: Actual capacity

The required data is SOC and P_{BESS}. When rainflow counting was applied to the SOC, it returned the DOD, index start, index end, and whether it was a half cycle or full cycle. For this analysis, the maximum DOD during discharge was identified from the results. Then, the corresponding indexes were used to locate the relevant time period in the power curve, and energy was then calculated through numerical integration.

Results and Discussion

Section 4.1, presents the outcomes from the data handling process are, which include the extraction of relevant data and the separation of the power curve into charging and discharging curves. Section 4.2 presents the RTE of the system, while Section 4.3 shows the results of a detailed efficiency analysis that provides a detailed explanation of the losses related to the operation of BESS. Section 4.4 will discuss parameters affecting the RTE, including an examination of the impact of missing data, SOC differences, and temporal resolution. Then influencing factors for operational conditions are presented in Section 4.5, which describes how operational conditions such as energy input, average SOC, idle period, and P-rate are related to system efficiency. Section 4.6 contains a suggested approach for determining BESS efficiency, and Section 4.8 presents the final discussion. In the following discussions, there is a differentiation between the system efficiency and the calculated system efficiency.The calculated system efficiency is referred to the BESS RTE and may deviate from the system efficiency due to issues related to data quality and other factors.

4.1 Data Handling

The time series data, described in Section 3.3, are used for this analysis and consist of real-time measurements obtained from the system depicted in figure 3.4. There are two overlapping data sets: Set1, with minute-resolution data spanning over a time period of 25 days, and Set2 with hourly data, spanning over a time period of 10 days. The values in Set2 are derived from Set1 and contains additional BMS data. Figure 4.1 is a scatter plot of the raw data of P_{BESS} from Set1 and Set2 for the same time period. Both sets were extracted from Pixii's database. A control calculation shows that the data in Set2 represents the average value for each 60-minute interval within Set1. The data is prepared just as described in Chapter 3. Figure 4.1 shows that P_{BESS} is zero until halfway through 2022-04-04, also called Day 4. In addition to this, the data on Day 15 in Set2 is incomplete. Therefore, only data between Days 5 and 14 will be used from Set2, while data from Days 5 to 30 will be used from Set1. In order to acquire the E_{BESS}, the power curve is separated into charging and discharging curves; this is done by following the strategy proposed in Section 3.3.2. This is applied for Set1 and

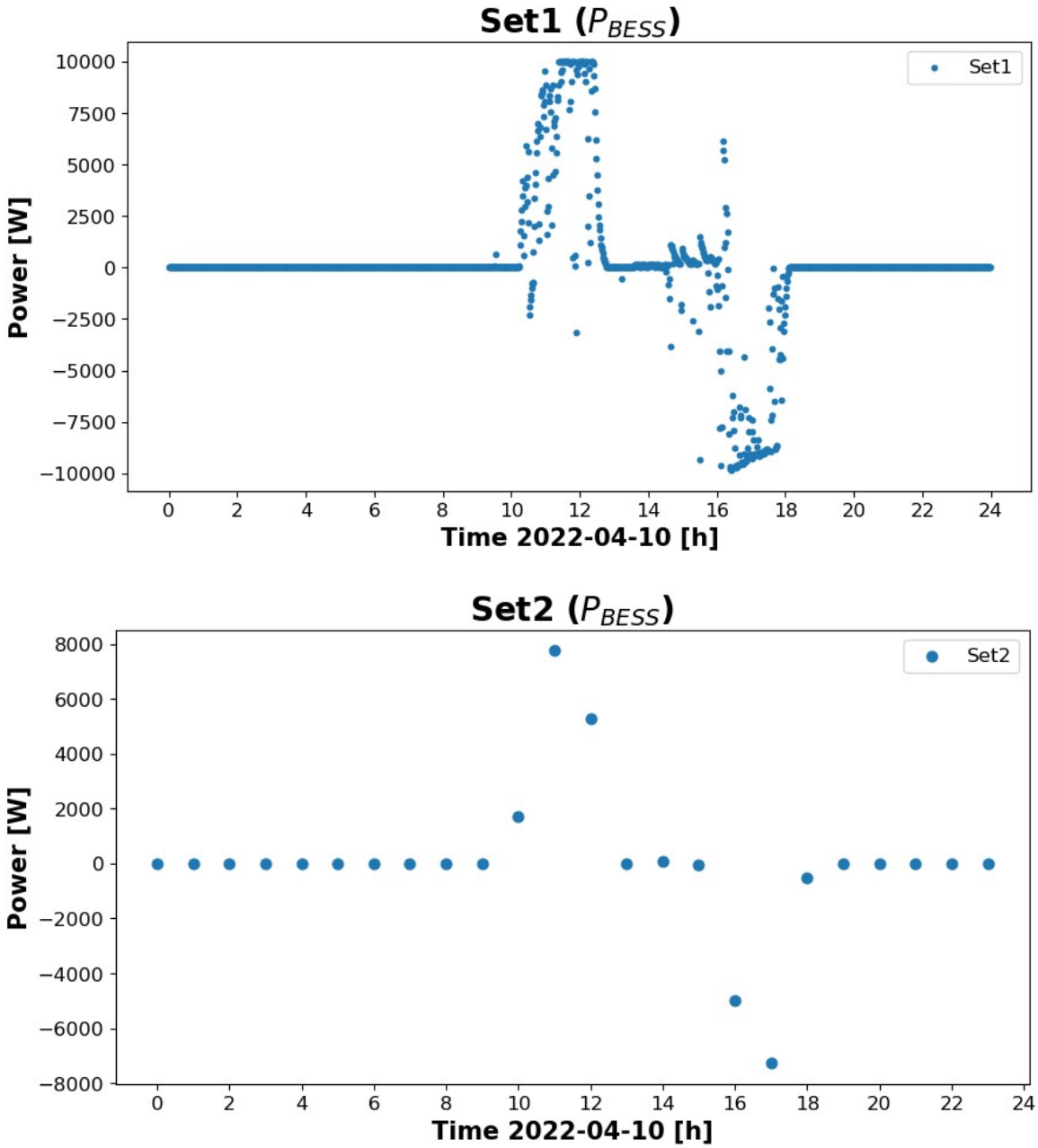

Figure 4.1: Scatter plot illustrating P_{BESS} in minute-resolution (top) and hourly resolution (bottom) for the same time period (2022-04-10).

Set2 on both P_{BESS} and $P_{Battery}$. An example of the curves after separation of P_{BESS} is illustrated in figure 4.2.

The SOC curve relates the state of BESS and provides important information on the battery's behavior during each state. When the battery is charging, the P_{BESS} is positive, and when discharging, P_{BESS} is negative. Figure 4.3 is the SOC curve of the battery from Set2 with the states defined as described in 3.3.2.

The BMS data does not provide $P_{Battery}$ and this value is therefore calculated us-

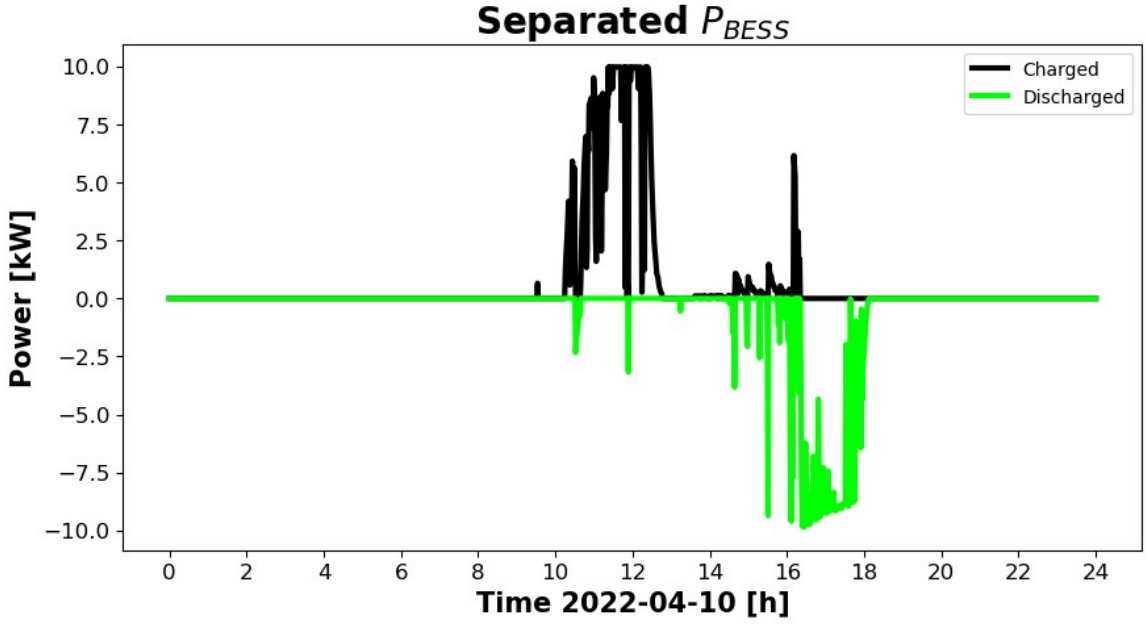

Figure 4.2: Illustrates the results when applying the curve splitting algorithm described in Section 3.3.2. The black curve represents the part where the BESS is charging, and the green curve represents the part where the BESS is discharging. Any irrelevant regions for each part were set to zero.

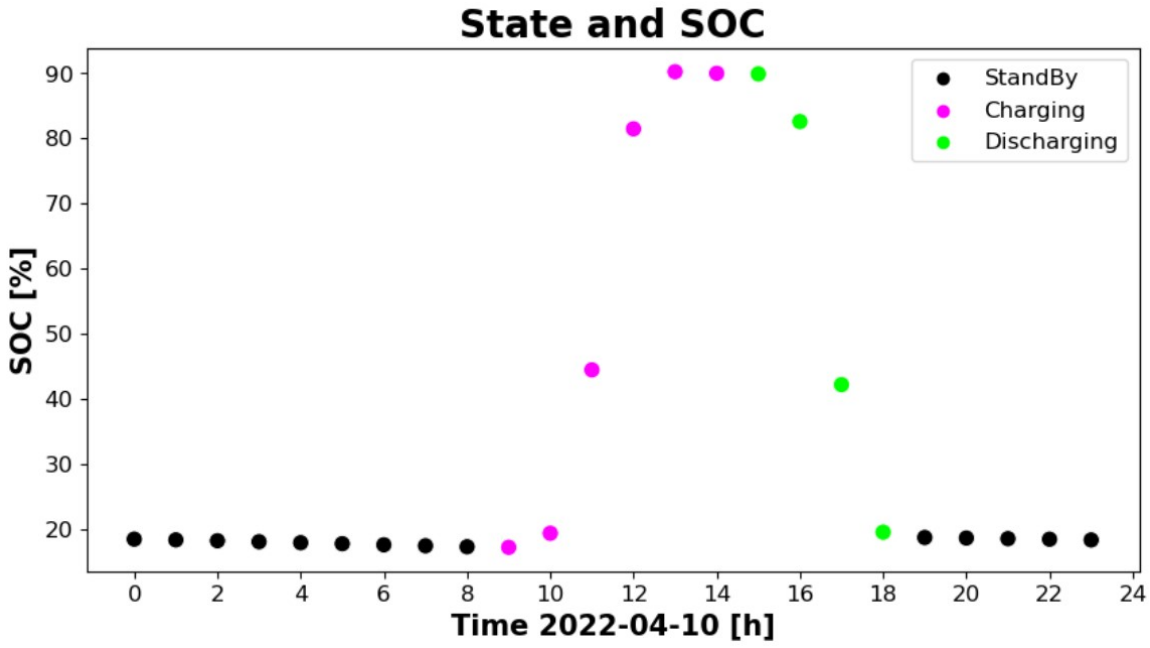

Figure 4.3: Depicts the state of BESS, defined in Section 3.3.2, on the SOC for 2022-04-10. Possible states for BESS are standby (black), charging (pink), and discharging (green). Hourly data (Set2) was used for illustration purposes.

ing voltage and current. Although it is common to approximate a constant value for the voltage, it is not accurate since the voltage varies proportionally with the SOC. This can be seen in figure 4.4 which shows the normalized values for voltage and SOC and the strong correlation between the two variables. Based on this, it is clear that to

get accurate values of the $P_{Battery}$, it is necessary to use the voltage that corresponds to the current for each hour. The dataset was partitioned into daily intervals. This approach was adopted because the daily curve's profile demonstrated minimal SOC variation between the initial and final points, which correspond to midnight of the relevant day and midnight of the following day, respectively.

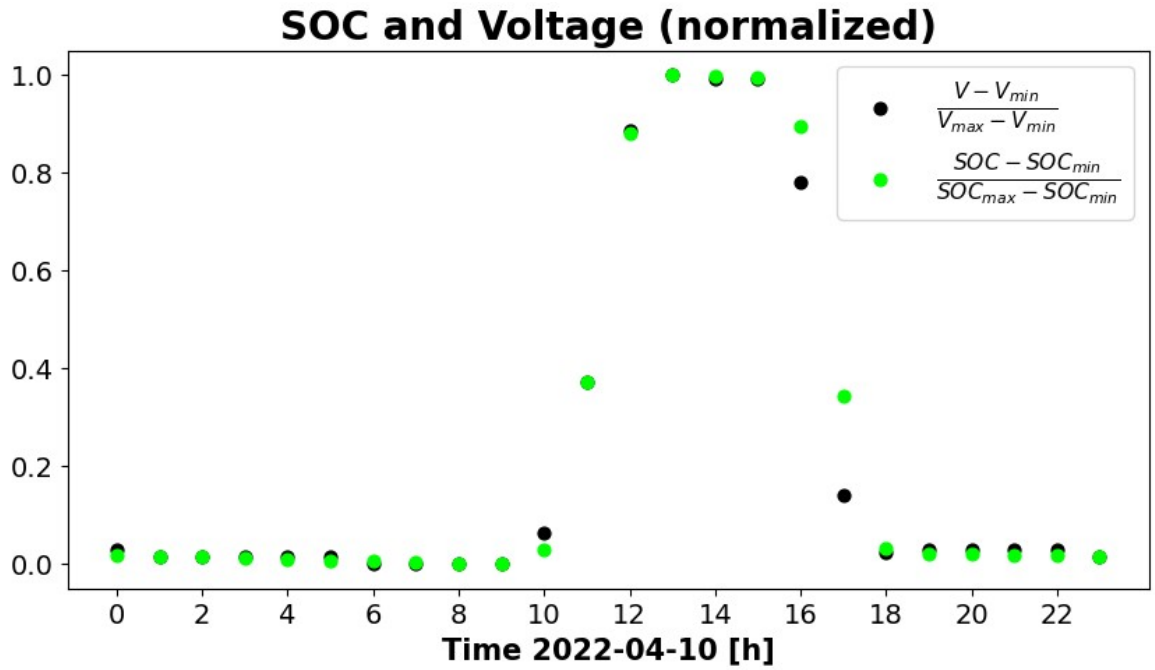

Figure 4.4: Shows normalized values for SOC and battery voltage to illustrate dependence. The two parameters are strongly dependent, and one estimation for a constant value of the voltage would be an inaccurate representation.

4.2 System Efficiency

The efficiency analysis will initially be conducted on a day that performs the expected operation, which is represented by the performance of a full charge cycle. This means that the BESS is charged until the maximum effective SOC. Day 10, depicted in figure 3.3, is used to represent the expected curve for this particular application. The SOC

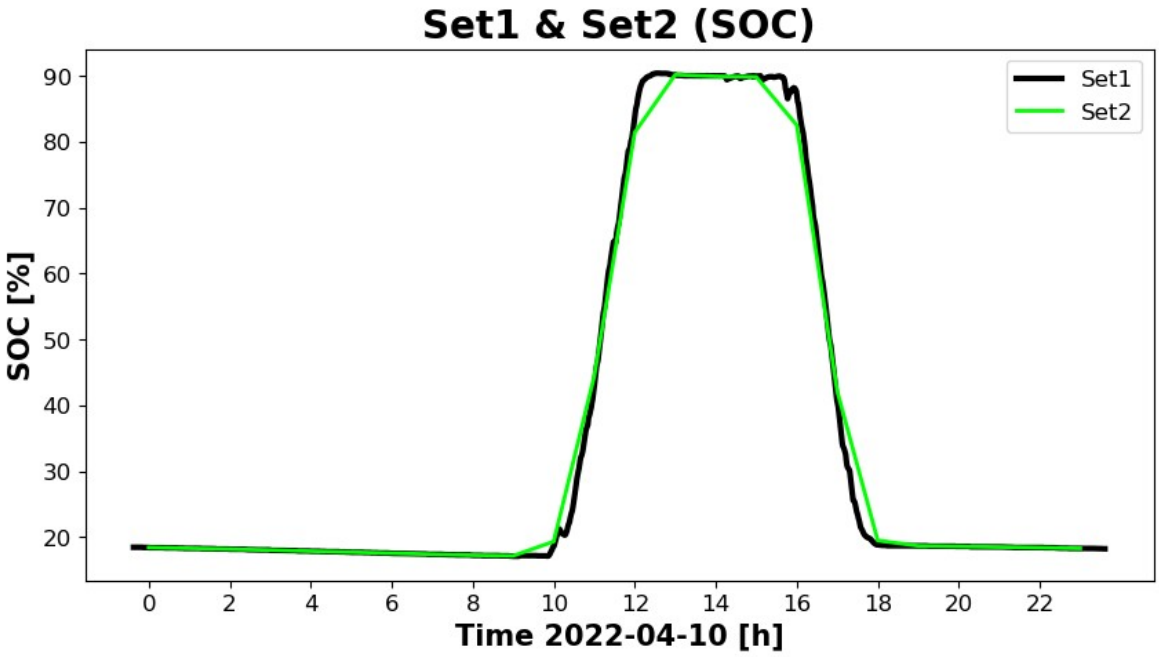

Figure 4.5: A comparison between the SOC curve from values in minute-resolution (black) and hourly resolution (green) for the period 2022-04-10.

curve will have one peak where the BESS charges from PV/grid when electricity prices are cheap and demand is low, around 10.00, and discharges when PV production is low and demand is high, around 18.00. The battery charges to its maximum effective SOC, but discharges just above the lowest possible effective SOC to account for potential losses during standby. The RTE in minute-resolution, shown in Table 4.1, is $\approx 85\%$, which is $\approx 15\%$ energy loss relative to the energy input.

BESS Roundtrip Efficiency	
ε_{BESS} [%]	84.7

Table 4.1: RTE for BESS in the period 2022-04-10 based on minute-resolution (Set1).

4.2.1 Discussion

The RTE, representing the system efficiency, is not only dependent on the battery's efficiency but also on the efficiency of the power electronics and the auxiliary system.

In this case, the losses due to auxiliary subsystem power consumption are considered to be baked into the RTE.

The study by [11] conducted a comprehensive literature review to estimate the RTE of BESS in PV applications. Their findings indicate that the efficiency ranges between 85-95%, but they did not specify the application or operating conditions. In contrast, [14] performed a more detailed efficiency analysis that accounted for 18 loss mechanisms related to different subsystems. Their estimation for BESS in PV applications was 84% when considering similar loss mechanisms as those in this study. The results on RTE in Table 4.1 align well with other literature findings. However, this number only provides an estimation of the total losses, determined using one day of operation, and the distribution of losses within the BESS remains unknown using this simple approach.

4.3 Detailed Component Efficiency Analysis

By applying the detailed component efficiency analysis proposed in Section 3.4, a more detailed insight into energy losses is provided. To conduct this analysis, BMS data is necessary. As BMS data is only available in aggregated format, it is essential to determine the deviation in RTE between minute and hourly resolution. The power curves in figure 4.1 show the difference between representation of BESSs power in the two data sets, and that Set 2 provides a less detailed description. Table 4.2 shows the RTE based on minute- and hourly data for the same time interval. The RTE

BESS Roundtrip Efficiency	Minute	Hour
ε_{BESS} [%]	84.7	86.4

Table 4.2: BESS RTE in 10-04-2022. Minute data is found in Set1, and hourly data is found in Set2.

when using hourly data deviates by 1.7%. Considering this deviation, the following results will only be discussed generally and approximately. The purpose will be to get a sense of how these losses are distributed without determining the actual losses at each component. The results from the detailed component analysis are shown in Table 4.3. Conversion losses in Table 4.3 refer to how much the RTE deviates from 100% efficiency. 'Power electronics' refers to the calculated losses during AC/DC (rectifier) and DC/AC (inverter) conversion. 'Battery' refers to total losses of the battery subsystem and is divided into two subcategories: losses when the BESS is in 'standby mode' and losses when the BESS is in operation; the category is named 'other'. In addition to the detailed component analysis, the battery efficiency, along with the voltaic and coulombic efficiency, is also calculated; the outcomes of these

Detailed Component Efficiency Analysis	
Conversion Losses[%]	13.6
Power Electronics[%]	10.55
Rectifier[%]	6.44
Inverter[%]	4.11
Battery[%]	3.05
Standby[%]	2.18
Other[%]	0.87

Table 4.3: Results of the detailed component analysis when applied to Set2, aggregated hourly data. The results show energy losses in each step, given in % relative to the energy input. The relevant time period is 2022-04-10.

calculations are presented in Table 4.4. The BMS data was utilized to compute the C-rate, revealing that the maximum C-rate for the entire period is 0.5.

Battery Efficiencies	
Energy η_E [%]	96.75
Coulombic η_C[%]	98.5
Voltaic η_V [%]	99.09

Table 4.4: Energy, coulombic, and voltaic efficiency of the battery subsystem in the time period 2022-10-04.

4.3.1 Discussion

Table 4.4 shows that the majority of losses occur during the conversion process, with AC/DC conversion resulting in slightly higher losses than DC/AC conversion. The study [14] found that the conversion losses considering only "inverter/rectifier" and "battery" totaled 15.7% where 13.2% were due to the actual conversion of the current and 2.5% were due to losses in the battery subsystem. The ratio between their conversion losses and battery losses resembles the same ratio as in Table 4.4. However, [14] estimated slightly higher losses related to power electronics, which may be due to their system's higher capacity and the type of application, which contributed to the greater impact of conduction and switching losses.

According to [14], the main contributors to losses related to the battery subsystem are "overvoltages, self-discharge, and losses in the battery connector." In this context, overvoltage refers to losses that occur during battery operation, while self-discharge refers to losses that occur when the battery is in standby. They also estimated that losses related to overvoltages or 'other' account for 2.4%, which is almost three times higher than the findings of this study 4.3. As discussed in theory, the magnitude of overvoltage depends on factors such as the C-rate, SOC, and temperature. Higher

losses resulting from overvoltage in [14] for the PV-BESS scenario could be due to their choice of application, which is frequency regulation. The application involves small SOC range cycles and requires a highly responsive battery to meet demand, potentially resulting in high C-rates.

According to [14], losses in the battery during standby were mainly due to self-discharge, which they estimated to be insignificant. However, the results in Table 4.3 show that the losses during standby for the BESS are much higher. This is because even when the BESS is in standby, the battery is still connected and therefore experiences a no-load current, which leads to standby losses. It is worth noting that the concept of self-discharge is typically used to describe the shelf life of a battery when it is disconnected, and is not commonly used to describe losses when a battery is connected to a circuit. This is also seen in the battery data specifications in Table 3.1 where it is specified that self-discharge is measured during storage.

Table 4.4 reveals that the battery's RTE falls within the expected range specified by the manufacturer, which is greater than 95%, as indicated in Table 3.1. Notably, [35] suggests that the battery RTE is significantly influenced by the C-rate. When the C-rate is ≤ 1, the anticipated RTE for charging or discharging is 97% or 95%, respectively. The voltaic efficiency, which is close to 100%, indicates that the battery voltage was stable throughout the operational period, implying small amounts of overvoltages. This observation is also in line with the results presented in Table 4.4. The measured coulombic efficiency of 98.5% reflects losses associated with chemical processes inside the battery cell. This value falls within the typical range of 95-99% reported for Li-ion graphite-based anode batteries [20]. In this study, these results have been useful in determining approximately if the different efficiency levels fall within the expected range. If the BMS data was minute-resolution, these results would be representative of the actual losses for each step, which would enable the investigation of energy losses tied to each subsystem.

4.4 Parameters Affecting System Efficiency Calculations

In this section, the impact of data quality and selected parameters on the RTE is explored. The SOC profiles of minute data are investigated to identify days that deviate from the expected operation and examine the curve characteristics that can result in reduced consistency or computational accuracy. Figure 4.6 presents a scatter plot of SOC curves, segmented into weekly categories that correspond to the actual weeks in

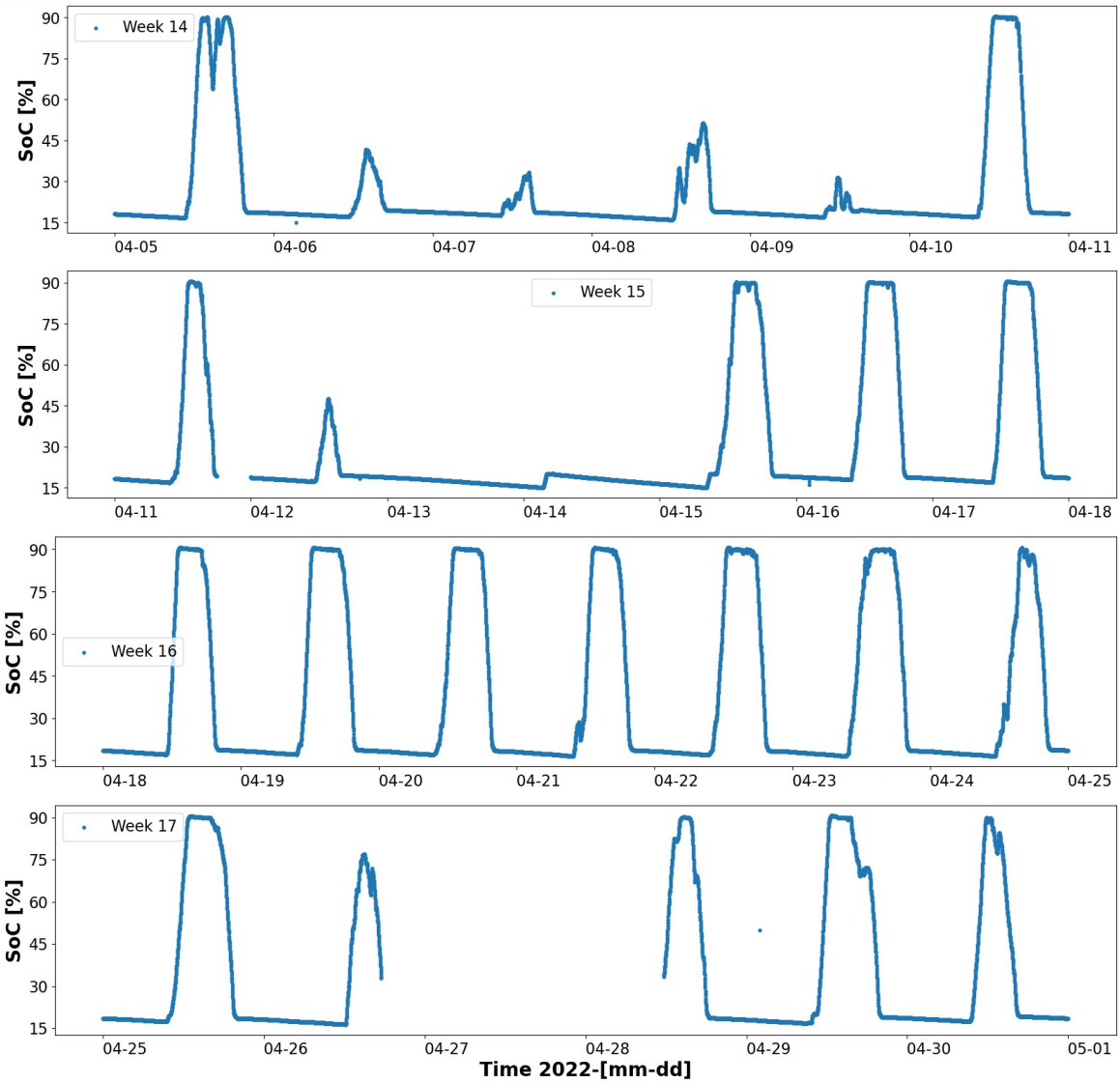

Figure 4.6: A comprehensive illustration of the SOC curve in the period between 1 and April 2022. The SOC values are minute data (Set1). The x-axis depicts the beginning of each day in April 2022. Each plot represents the corresponding week, starting with week 14 at the top and ending with week 17 at the bottom.

2022. Here, the negative slope during standby is better illustrated, which indicates standby losses that occur outside of operation. It illustrates that while the majority of days performed according to the expected operation, there are a number of days BESS did not reach full potential. This operational behavior is typically attributed to external factors, for example, variations in local weather conditions. Figure 4.6 shows that Week 14 contains the highest number of days that deviate from the expected operation, while Week 16 contains almost only days that perform as expected. Weeks 15 and 17 exhibit incomplete data, which is a commonly encountered issue during data collection. Missing data can compromise the accuracy and completeness of the dataset. This section is organized into three main components. Firstly, it examines the impact of missing data on RTE. Secondly, it explores how differences in SOC can

affect the resulting RTE. Finally, it delves into how data resolution can influence the interpretation of various types of curves.

4.4.1 Missing Data

Missing data can arise due to various reasons, including measurement errors or the disconnection of the battery for maintenance purposes. In minute data, missing data is observed in two instances: a brief time period on Day 11 and a much longer duration spanning Day 26 to 28, as depicted in Figure 3.3. The expected count for complete daily data is 1440/1339 minutes. Any deviations from this expected count would indicate missing data. The primary concern with missing data is the loss of relevant information during the affected period. Therefore, it is important to determine the extent of information loss before it significantly impacts the accuracy of the calculated RTE. The RTE for Days 11, 26, and 28 is shown in Table 4.5.

April 2022	11	26	28
BESS RTE [%]	85	72	109

Table 4.5: RTE of 2022-04-11, 2022-04-26 and 2022-04-28, periods with significant missing data.

4.4.1.1 Discussion

The findings in Table 4.5 shows the weakness of using the approach shown in Section 4.2 to calculate RTE. With this method, an apparent RTE exceeding 100% is found, which suggests that the system gained energy during the conversion process. This is because the SOC curve starts with a higher SOC and discharges to a lower point than its initial point, meaning that the BESS was able to discharge more than it charged, resulting in an efficiency greater than 100%. Similarly, on Day 26, the calculated efficiency is lower than expected, which can be explained by the fact that the initial point is much lower than the end point, indicating that the BESS charged more than it discharged. These results demonstrate the importance of ensuring that the initial and end points in the SOC curve match in efficiency calculations.

However, for Day 11, despite some missing data, the RTE calculations for Day 11 align with the expected RTE, indicating that the impact of missing data is contingent on its location in the data. In this case, the missing data is located in the standby region, between two points where it is expected to be a continuous slope. This allows the numerical integration algorithm to accurately estimate the shape of the gap, typically by using linear estimations. In conclusion, in order to include incomplete time periods, the missing data cannot contain important information on the operation. If it occurs

when the BESS is expected to be in operation, then the entire time period is irrelevant for RTE, since it will contribute to inconsistency. However, if the missing data occurs outside of operational hours, the time period can still be used for estimating system efficiency.

To ensure the integrity of the results, days that lack crucial information about the SOC curve, such as Days 26 and 28, are disregarded for the remainder of this chapter. However, days that lack non-crucial information, such as Day 11, are included in the analysis.

4.4.2 SOC Difference

The SOC difference is defined as the variation between the start and end points of the relevant SOC curve, and its significance in accuracy calculations were discussed in section 4.4.1. When the SOC difference is considerable, the curve becomes unsuitable for BESS efficiency analysis. However, certain days exhibit relatively lower SOC differences, such as Day 15, and could possibly still be used for BESS efficiency analysis. This section aims to investigate whether the RTE of such profiles can still be considered reliable and to compare various strategies to correct for the SOC difference.

The SOC difference for Day 15 is 2.6%, and the corresponding RTE is 82.2%. Nonetheless, as shown in Figure 4.7, the SOC on Day 15 exhibits expected behavior, and one would expect an efficiency of $\approx 85\%$. As demonstrated in the "missing data" section, a positive SOC difference implies that the battery was discharged less than intended, resulting in a calculated efficiency lower than the expected efficiency. Three proposed methods for SOC correction will be used to investigate if this deviation is due to the SOC difference. The primary goal of the first two methods is to determine the energy equivalent to the SOC difference and include it in the calculations. The last method identifies the closest point where the SOC difference is less than 1 %, preferably in the idle period when the E_{BESS} is zero. The values of $E_{BESS-in}$ and $E_{BESS-out}$ are 18.86 kWh and 15.49 kWh, respectively.

4.4.2.1 Method 1 and 2

The value for $SOC_{diff} = 2.6\%$ is inserted in both method 1 and method 2 in the calculations described in 3.5.1. The energy corresponding to the SOC difference is $E_{SOC_{diff}}$= 508Wh according to method 1 and $E_{SOC_{diff}}$= 650Wh according to method 2. After adding the estimated energy to the $E_{BESS_{out}}$ the corrected efficiencies for method 1 and method 2 becomes $\varepsilon_{corr} = 84.8\%$ and $\varepsilon_{corr} = 85.6\%$, respectively.

4.4.2.2 Method 3: SOC Correction Algorithm

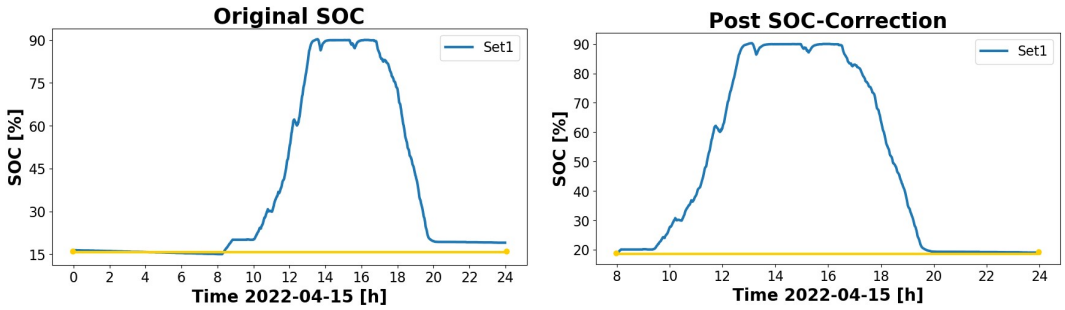

Figure 4.7: The SOC curves from minute data (Set1) for 2022-04-15 original (left) and post-SOC correction (right) The yellow line shows the SOC difference between the start and end points.

Method 3 is applied to Day 15, reducing the SOC difference from 2.6% to 0.4% and resulting in a corrected efficiency of $\varepsilon_{corr} = 85\%$. The curve before and after SOC correction is shown in Figure 4.7. The results of all three methods are summarized in Table 4.6.

April 2022 Day 15	Original	Method 1	Method 2	Method 3
BESS RTE [%]	82.2	84.8	85.6	85 .4
SOC$_{t1}$-SOC$_{t0}$ [%]	2.6	0	0	0.4

Table 4.6: A summary of the RTE before and after using the proposed correction methods for SOC difference, along with the corresponding SOC difference.

4.4.2.3 Discussion

Three methods were presented to correct for the SOC difference, including method 1, which estimated energy from the nominal capacity in the data sheet; method 2, which estimated energy from the actual SOC curve; and method 3, which employs the SOC algorithm described in Section 3.5.1. The three methods generated approximately the same results for RTE corrections, which also represent a value closer to the expected RTE value, indicating that the SOC difference did have a significant impact on RTE calculations and that even a small SOC difference of 2.5% will contribute to inaccurate RTE.

Although the first method is the simplest and most straight-forward, it does not account for battery degradation and becomes less accurate over time. The second method is independent of nominal capacity and uses the trend of the curve itself, which removes uncertainties related to capacity fade and is based on realistic operational factors. The third method is the most reliable since it does not rely on estimations and instead identifies a point in the same interval where the SOC difference becomes negligible ($<$1%).

In order to use this method effectively, the new estimated interval should not exclude important information about the BESS operation. In this case, the new SOC interval mostly excluded time periods where the BESS was in standby.

The maximum threshold of SOC difference for SOC correction will depend on the application type. In this application, it was possible to apply SOC correction for up to 2.6% SOC difference, without losing a significant amount of essential information, which allows the RTE for this day to be included in a performance evaluation without affecting consistency. The SOC difference exhibited on Days 26 and 28 is an example of a not-correctable SOC difference, while the SOC difference exhibited on Day 15 is an example of a correctable SOC difference.

4.4.3 SOC Difference Overview

Now that it is established that even a small percentage of the SOC difference can have a significant impact on the accuracy of RTE, it is interesting to map out the potential impact of the SOC difference on RTE for the available time period. Figure 4.8 provides an overview of the SOC difference for each day, with the SOC differences plotted against the corresponding RTE. Day 13 and 14 are not included due to zero energy input, and Days 26 and 28 are not included due to a 15% SOC difference. Each point is marked with a day number referring to the equivalent day in April 2022.

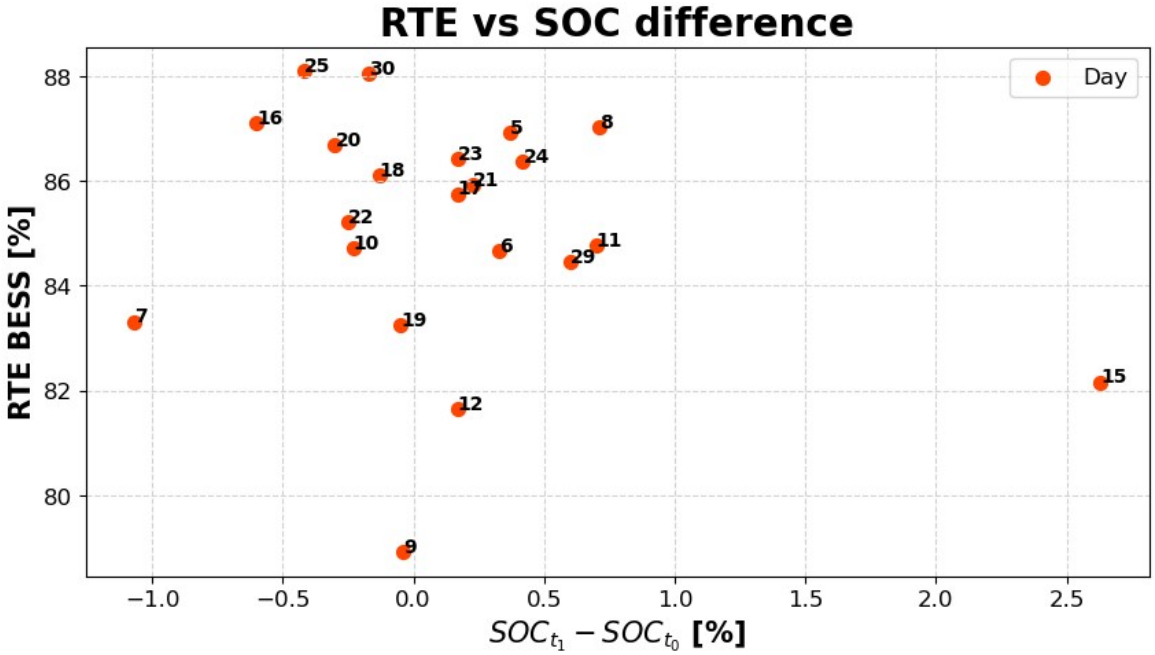

Figure 4.8: The relationship between RTE and SOC difference for BESS in April 2022. Each point is assigned to the corresponding day.

4.4.3.1 Discussion

The results show that there are two clear outliers: Day 15, which has been discussed, and Day 7, which has a negative SOC and shows that the RTE is estimated to be higher than expected. Figure 4.6 shows that Day 7 is a low input day very similar to Day 9, and one expects both to have lower efficiency than days with full charge cycles. The unexpectedly high RTE of Day 7 can be related to the negative SOC difference.

As for the other RTE calculations, the SOC difference is generally $<|1\%|$. Even for these results, a slight difference is seen between negative and positive SOC differences. The negative SOC differences have a slightly higher RTE than the positive SOC differences, even though, based on the SOC curve in Figure 4.6, the BESS operate similarly. This shows the effect of the SOC difference on the accuracy of RTE, even when the SOC difference is $< 1\%$. Days with a negative SOC difference may result in a slightly higher RTE, and days with a positive SOC difference may result in a lower RTE.

4.4.4 Temporal Resolution

In Section 4.3, it was shown that the RTE from hourly data showed a slight deviation from the RTE from minute data. This section wants to see how this applies when operational behavior is changed. Since Day 9 is an example of a different operational behavior, it is suitable for this purpose. The RTE, on Day 9, from both data sets is shown in Table 4.7, which indicates that losses are 21% according to minute data and 40% according to hourly data. Although it could be interesting to get a more detailed efficiency analysis as done in Section 4.2, the results from hourly data deviate significantly from minute data, and applying the detailed component analysis is irrelevant in this case.

April 2022 Day 9	Minute	Hour
BESS RTE [%]	78.92	60.44

Table 4.7: A comparison between BESS RTE when using minute data (Set1) and hourly data (Set2). Illustrating the impact of temporal resolution. The relevant time period is 2022-04-09.

4.4.4.1 Discussion

The efficiency for Day 9 shows that the losses relative to energy input are greater for this day compared to the days with full charge and discharge cycles. This is mainly due to the low input, which causes losses to have a larger impact on the ratio calculation. This effect is illustrated and discussed further in [22]. Another reason for this could be attributed to the fact that the accuracy of numerical integration is

directly proportional to the number of data points used to describe the actual curve, or, in other words, the temporal resolution. Although aggregated data is intended to be representative of the values, it may not accurately represent the shape of the curve, which is a crucial factor during numerical integration. This causes the numerical integration algorithm to estimate the curve shape between each data point, which may not always be accurately representative.

4.4.5 Temporal Resolution Overview

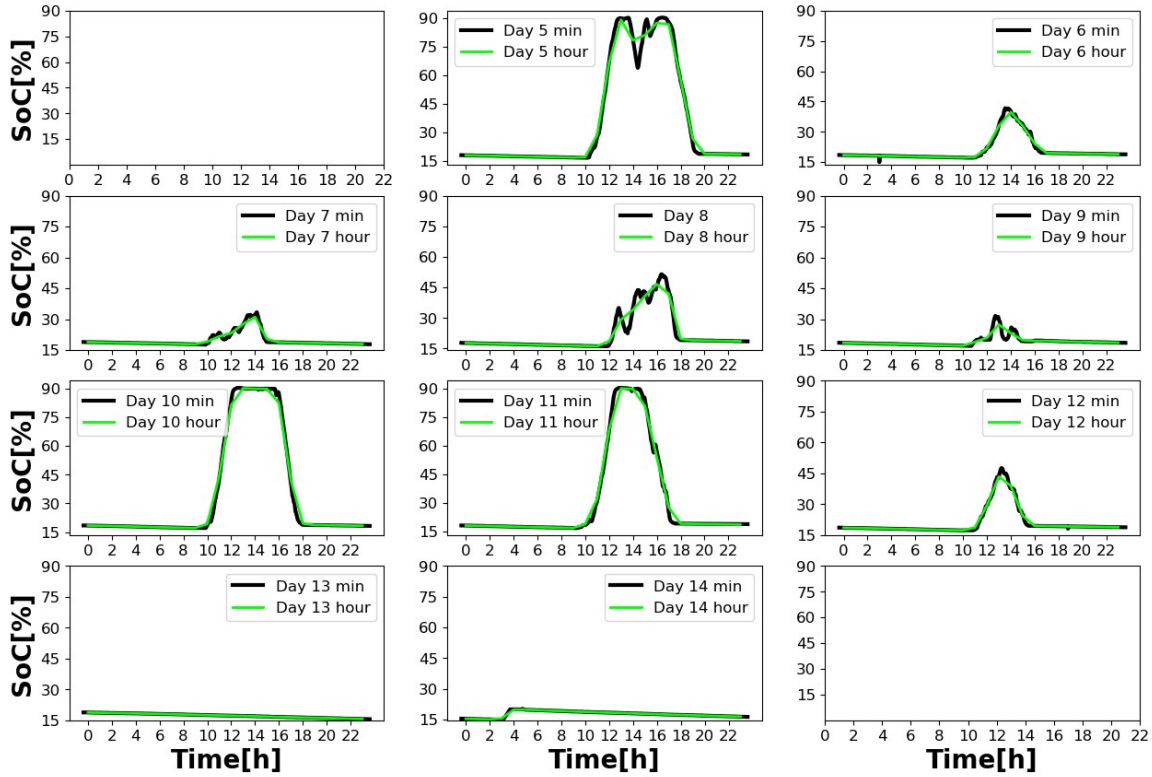

Figure 4.9: A comparison between SOC values in minute data (black) and hourly data (green) and depicts daily SOC curves for April 5–14.

It would be interesting to investigate which factors may contribute to inaccuracies in low-resolution data. This section aims to further investigate the impact of resolution, building upon the discussion presented in Section 4.4.4. To accomplish this, efficiency calculations were applied to each day in the period between April 5 and April 14. Figure 4.9 illustrates the differences in SOC curves for minute- and hourly data; for details on the actual values of RTE, SOC difference, energy input, and energy output, see Table 6.1 in Appendix 1. In an attempt to see the different impacts of temporal resolution, minute data is aggregated by taking the mean value for different time spans: 20 minutes, 40 minutes, and 60 minutes. Figure 4.10 shows the RTE for minutes and aggregated data for time intervals up to 60 minutes.

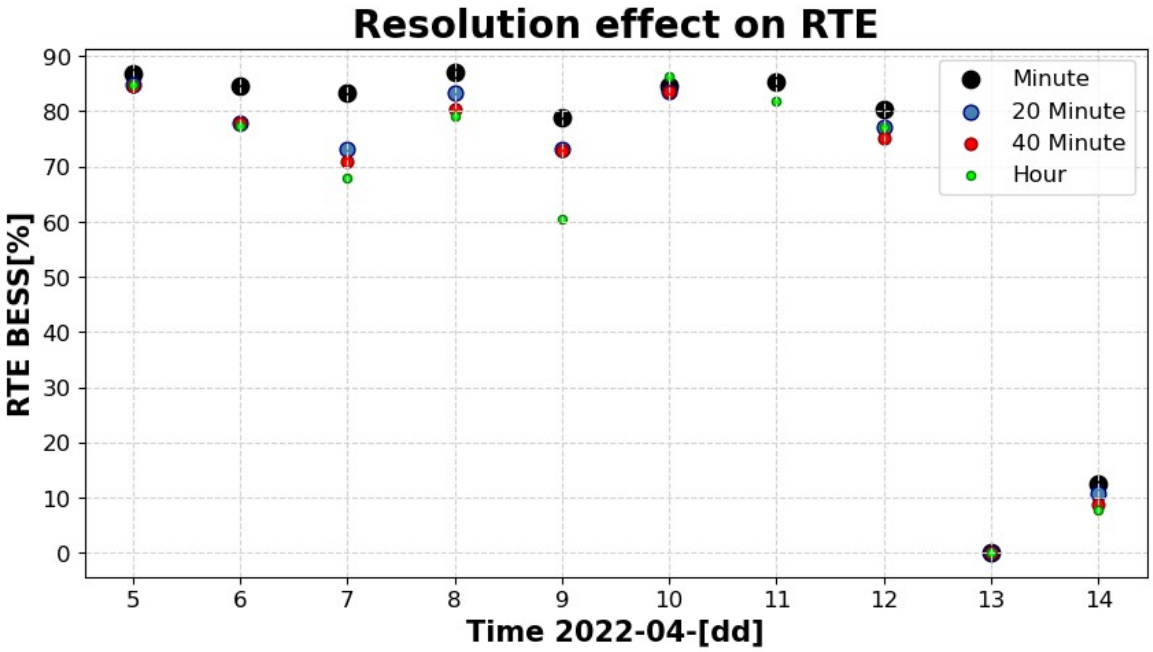

Figure 4.10: An illustration of the impact of temporal resolution on RTE. There are 4 resolutions evaluated: 1-minute intervals (black), 20-minute intervals (blue), 40-minute intervals (red), and 60-minute/hour intervals (green).

4.4.5.1 Discussion

Figure 4.9 shows that, generally, Set2 estimated the SOC curves representatively. However, when examining days with high frequency peaks, such as Days 5 and 8, it shows that for these Days, the aggregated data will not be able to describe the shape of the SOC curve as efficiently. According to the apparent difference, seen in Figure 4.9, between minute- and aggregated data, it is expected that the deviation in Days 5 and 8 would be similar to Days 7 and 9, but the impact from resolution is higher for Days 7 and 9. Table 6.1 shows that this can be attributed to the fact that when the input and SOC range are higher, the error due to resolution has less impact. It is important to note that a high SOC range and high input are related, as the BESS is programmed to mainly charge during one hour and discharge during another hour. Therefore, typically, a larger SOC range implies more energy input. Figure 4.10 indicates that the smallest deviation between minute- and aggregated-data is observed for Days 5, 10, 11, and 13, which share similar characteristics such as a similar SOC range and high input. The exception is Day 13, which exhibits zero energy input and output. On the other hand, the largest deviation is observed for Days 7 and 9, which share characteristics of a significantly reduced SOC range and low input.

In conclusion, the resolution seems to have a larger impact on days with low input and average SOC, since deviance in RTE will be larger when energy input is lower. If lower-resolution data is applied, the requirements for higher input and an average

SOC range need to be more strict.

4.5 Impact Of Operational Parameters On System Efficiency

After assessing the data quality of BESS efficiency calculations, an investigation of external operational conditions that impact system efficiency must be conducted. In Chapter 2, an overview of the loss mechanisms in the BESS and its subsystem was provided, and the influencing factors for each loss mechanism were summarized in Table 2.2. Among these were power input, C-rate, SOC level, and idle periods. This section aims to provide an in-depth analysis of these factors and their specific effects on system efficiency.

For this section, only minute data will be used, and days that exhibit more than a 1% SOC difference will be disregarded. Additionally, days that have less than 1 kWh of input will also be excluded from the analysis. Only days with complete datasets containing all 1440 minutes will be used, as this enables consideration of not only the shape of the power curve but also other properties such as BESS idle periods and average SOC.

4.5.1 Energy Input

For this application, the power input affects the SOC range, with a higher input resulting in a higher average SOC. It also impacts the idle period, as higher power input leads to longer operating hours and a decrease in the idle period. Furthermore, low power input creates a SOC profile that is sensitive to low data quality, as discussed in Section 4.4.5. In the following analysis, the energy input represents the power input for each day. Figure 4.11 displays the energy input per day plotted against the corresponding RTE to illustrate the relationship between energy input and system efficiency, with each point labeled by its day number.

The C-rate is an important characteristic of power, and it denotes the speed at which the battery charges. Literature suggests that the C-rate is associated with an increase in both overvoltage and internal resistance. Losses are typically evaluated by examining the C-rate; this is because the P-rate will also include fluctuations in the voltage, which makes it a more complicated variable. Since BMS data, which contains recordings of the current, is not available in minute-resolution, the available parameter for evaluation becomes P_{BESS}, which necessitates an investigation of the power rate instead. Based on the high voltaic efficiency, indicating small fluctuations in the volt-

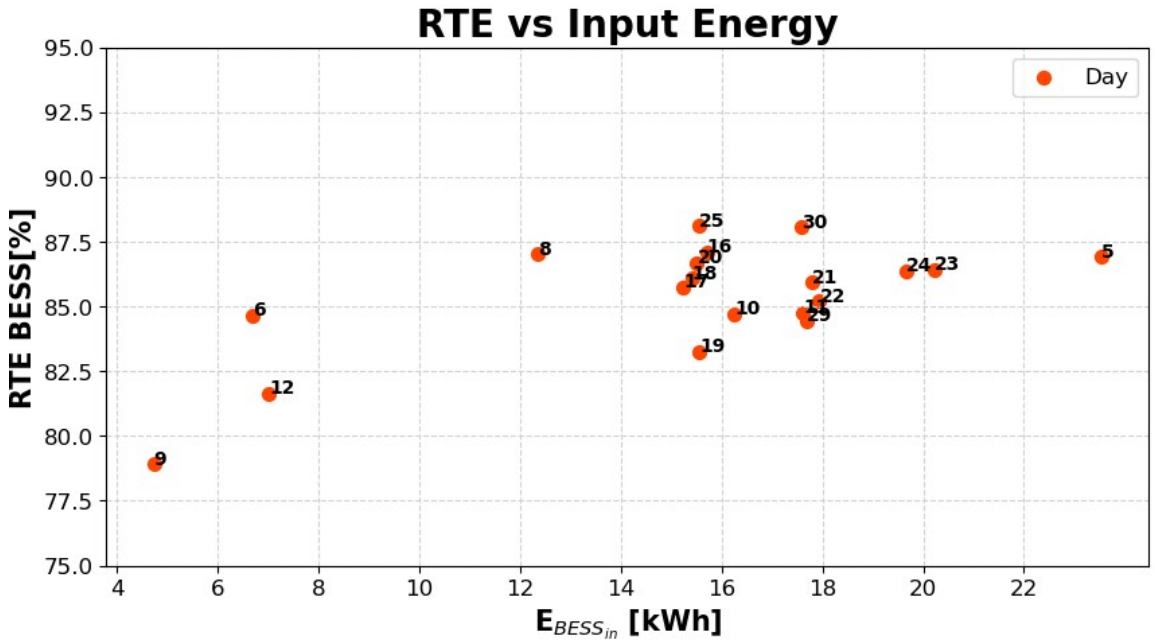

Figure 4.11: The relationship between RTE and $P_{BESS_{in}}$ for BESS in April 2022. Each point is assigned to the corresponding day.

age and control calculations with Set2, the trends observed using the P-rate should be representative for the C-rate. Using the maximum P-rate for each day serves as a representation of the P-rates per day. Figure 4.12 shows the maximum P-rates for each day, separated into P-rates for the charging and discharging curves.

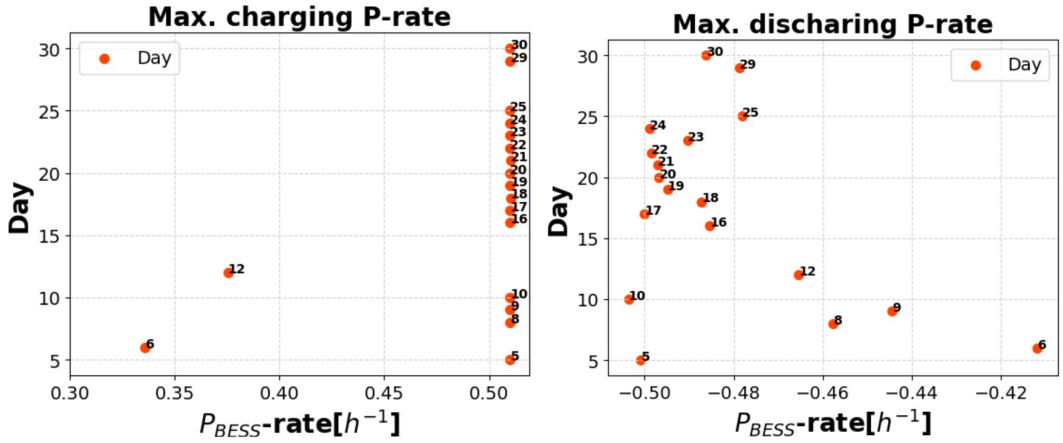

Figure 4.12: The maximum P-rate using P_{BESS} for charging (left) and discharging (right) Each point is labeled with the corresponding day.

4.5.1.1 Discussion

As shown in Figure 4.11, there is a positive correlation between energy input and RTE. Day 9 is the day with the lowest energy input and RTE. However, the opposite is not necessarily true. Although Day 5 has the highest energy input, it doesn't have the

highest efficiency. Figure 4.6 reveals that Day 5 is a day with full charge, but also exhibits a higher frequency of operation compared to the expected behavior. This means that the BESS was fully charged as expected, and then there was additional energy input during the other peaks. According to [34], higher power input results in decreased BESS efficiency due to an increase in internal resistance. This is confirmed in Table 6.1 which shows that Day 5 had the highest energy losses. However, according to [22], higher power input contributes to making conversion losses less significant. This is seen when comparing losses on Days 5 and 9. Day 9 has the lowest energy losses of 1 kWh, while Day 5 has the highest energy losses of 3 kWh. However, Day 9 is a low input day, making these losses highly significant, while Day 5 is a high input day, making the losses less significant. This proves that the energy losses have less effect when the input is higher, as discussed in Section 4.4.5.

Figure 4.12 demonstrates that the maximum charging P-rate per day remains constant at 0.5 for most days, except for Days 12 and 6. The SOC curve in Figure 4.6 shows that these are days with small charging cycles, and 4.11 illustrates that the power input is low and may not have been sufficient to achieve a P-rate of 0.5. In contrast, the discharging P-rate exhibits a greater degree of variation, which may be attributed to its dependence on inconsistent load conditions. Specifically, days with full charging cycles characterized by smooth curves have a maximum P-rate of 0.5, while Days 30, 29, and 25 exhibiting full charge days with irregular operation fail to reach a maximum P-rate of 0.5. Additionally, previous literature has suggested that system efficiency is influenced by charging and discharging rates. Indirectly, higher P-rates can lead to increased internal resistance and greater losses, although this effect cannot be conclusively determined in the present study due to P-rates that do not exceed 0.5, and most literature on this topic has focused on losses associated with C-rates exceeding 1, such as [35].

In conclusion, although higher energy input is associated with higher energy losses, the impact of energy losses on BESS efficiency decreases when energy input increases. The p-rate for this application is 0.5, indicating limited losses. The charging P-rate shows that the BESS is able to reach maximum P-rate when charging, but this is not always true when discharging.

4.5.2 Average SOC

The average SOC provides insight into which SOC levels the BESS spent most time at. For example, a higher average SOC indicates that the BESS spent more time at high SOC levels. In this application, the average SOC reflects the SOC range for the

relevant time period, and a higher average SOC corresponds to a larger SOC range. This is because the BESS fully discharges at the end of each day, regardless of how much it was charged. Figure 4.13 shows the average SOC for each day plotted against the daily RTE, with each point labeled by the respective day.

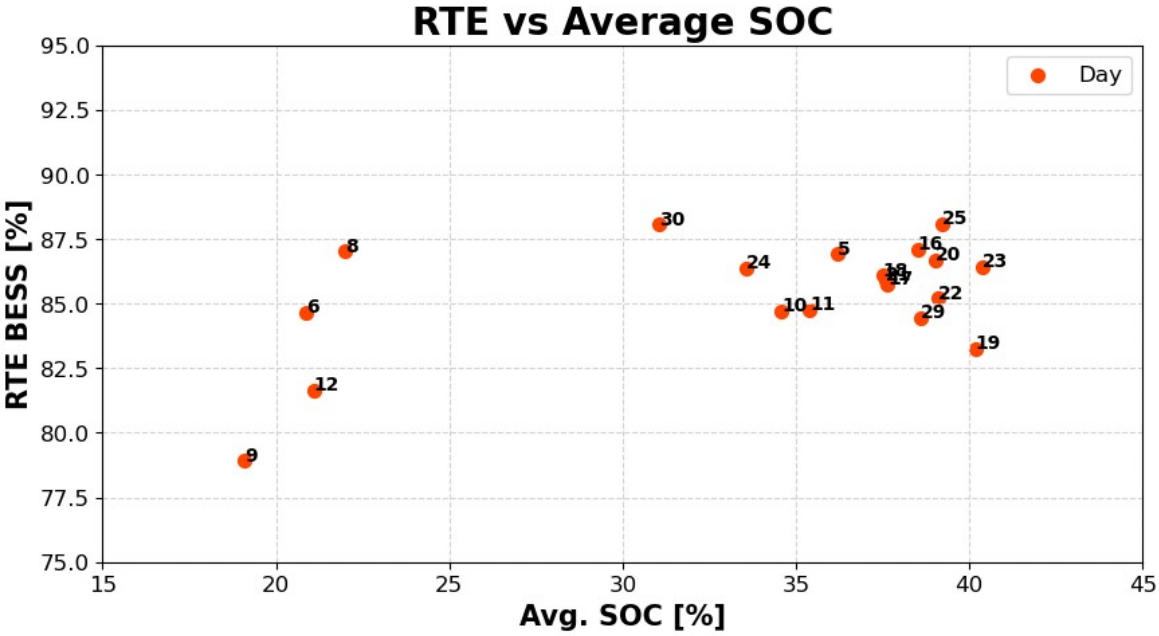

Figure 4.13: The relationship between RTE and the average SOC for BESS in April 2022. Each point is assigned to the corresponding day.

4.5.2.1 Discussion

Figure 4.13 illustrates a clear distinction between the average SOC of high and low efficiencies. In particular, Days 6, 8, 9, and 12, all characterized by low energy input, have the lowest average SOC, just as expected. Days that charged to maximum SOC, which represent the expected operational behavior, have an average SOC between 30 % and 40 %, including Day 10 with an average SOC of 35 %. The average SOC vs. RTE plot in [14] revealed a significant difference between low and high SOC ranges. This study shows similar results; Figure 4.13 shows that low SOC ranges corresponded to days with lower RTE and high SOC ranges corresponded to days with higher RTE. The correlation between low and high average SOC and RTE is not necessarily due to the influence of SOC level on the internal resistance of the battery; rather, it is due to the correlation between energy input and average SOC, as discussed earlier. On the lower end of the interval for days operating at full capacity, are Days 24 and 30, which show a narrower SOC curve, indicating that the BESS discharges sooner than expected. On the higher end, with slightly more than 40 % average SOC, there are Days 19 and 23, which have a wider SOC curve, which means that the BESS has high SOC levels for a longer period. According to [36] high SOC levels have a higher impact

on internal resistance compared to low SOC levels. This effect might be observed on Day 19, where BESS operated at full capacity just as expected, with a low SOC difference but an unexpectedly low RTE. Day 19 also exhibits the highest average SOC, indicating higher SOC levels for a longer period, which may be the main reason for its lower efficiency.

The average SOC is useful as it provides insight into the operation of the BESS. The knowledge of the correlation between average SOC and RTE, can be used to gain insight on how much the BESS experiences high or low SOC levels. In this case, it provided insight into typical SOC ranges for expected operations, which can make it possible to identify low operating days or deviating operations, such as Days 24 and 30, with narrower SOC curves, or Days 19 and 23, with wider SOC curves.

4.5.3 Idle Period

In Section 4.3, it was determined that a significant part of the battery losses can be attributed to the no-load current, which occurs when the BESS is in standby mode. The time that BESS spends in standby mode is referred to as the idle period. Figure 4.14 presents a plot of the idle period as a function of the RTE, used to investigate the significance of idle periods on system efficiency.

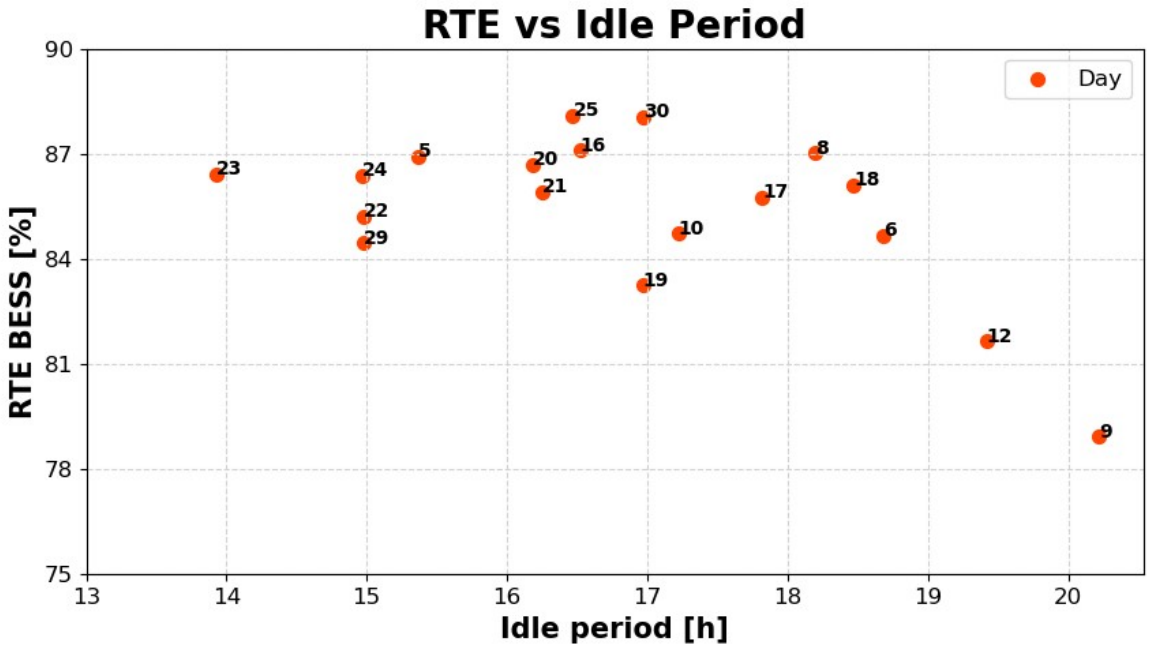

Figure 4.14: The relationship between RTE and idle periods in hours for BESS in April 2022. Each point is assigned to the corresponding day.

4.5.3.1 Discussion

As seen in Figure 4.14, the RTE will increase with decreasing idle periods for the low input days, while there will be no apparent correlation between days resembling the expected operation. This observation is both attributed to the higher losses incurred by BESS due to the continuous discharge during extended idle periods and the higher significance of energy losses on low input days. According to [22] the BESS efficiency increases when the system is constantly exploited, avoiding idle time or low power operation. For this application, according to Figure 4.14 the threshold separating expected and non-expected behavior is a maximum idle period of 18 hours. Another observation is that the SOC curves for days with a shorter idle period, 5, 24, 22, 29, and 23, all have fluctuations and irregularities at their peaks, indicating that it operated when it wasn't expected to. This represents a SOC with higher fluctuations, indicating a higher cycle frequency in operation.

In conclusion, the idle period describes how long the BESS was in standby mode and directly relates to the energy losses during standby. The correlation between a long idle period and RTE is apparent, and the idle period can be used as a tool to distinguish between days with expected operation and non-expected operation, as well as expected operation with irregularities.

4.6 Suggested Approach For Determining Battery System Efficiency

The findings in this study can provide valuable insights for determining BESS efficiency. Which can be used to conduct a performance evaluation. The approach used in this study involved establishing the influencing factors in order to gain consistent results for the RTE. The factors were energy input, which identifies non-operating days; average SOC, which identifies narrow or wide SOC curves; and idle periods, which identifies curves with irregular operation. It was discovered that the influencing factors can act as tools to describe different aspects of the operational conditions. These descriptive tools can be provided along with the RTE to give further insight into the operation of BESS. Another use case for these tools is to create requirements for different levels of performance. Table 4.8 shows two levels of performance for this particular setup. Level 1 applies less restrictive requirements; it allows for up to 3% SOC differences given that they are corrected by using one of the suggested methods; it allows for some missing data as long as it is in the non-operating region; it will disregard energy inputs less than 5 kWh in order to include only operating days; the average SOC includes the majority of days, disregarding the outliers on the lower

Requirements	**Level 1**	**Level 2**
SOC difference [%]	$\leq 1\%$	$\leq 1\%$
	& SOC-corr. ($\leq 3\%$)	
Missing Data [min]	≤ 1	≤ 1
	& If $P_{BESS} = 0$	
$E_{BESS_{in}}$ [kWh]	[←,5]	[14,22]
Average SOC [%]	[30,45]	[30,40]
Idle Period [h]	[←,18]	[15,18]
Days	14	7
BESS RTE [%]	**85.5**±2.5	**86.5**±1.5

Table 4.8: Two ways for defining requirements with different levels of restriction.

end; and the idle period is set to a maximum of 18 hours, disregarding the days with non-expected behavior. When these values are applied, the RTE becomes $85.5 \pm 2.5\%$. Level 2 applies more restrictive requirements; it is strictly set to only days with less than 1% SOC difference; no missing data is allowed; the energy input is restricted for both too high and too low values; the average SOC disregards extreme outliers on either end; and the idle period is restricted on both ends, disregarding days with non-expected behavior and days with an irregular SOC curve. The RTE for level 2 becomes $86.5 \pm 1.5\%$. This shows that the estimated RTE is dependent on how the requirements are defined. Although level 2 provides the advantage of reducing the variability in the results, which can improve the accuracy of the measurements, it comes at the cost of limiting the number of days available for comparison. On the other hand, level 1 allows for more variation in the RTE results but provides twice as many days that meet its requirements.

An attempt to summarize the entire process from raw data to estimating system efficiency through RTE is shown in Figure 4.15. The suggested requirements for the expected curve include an upper limit for SOC difference, an upper limit for missing data, a range for energy input, a range for average SOC, and a range for idle periods. The actual value for each requirement will vary depending on the type of application.

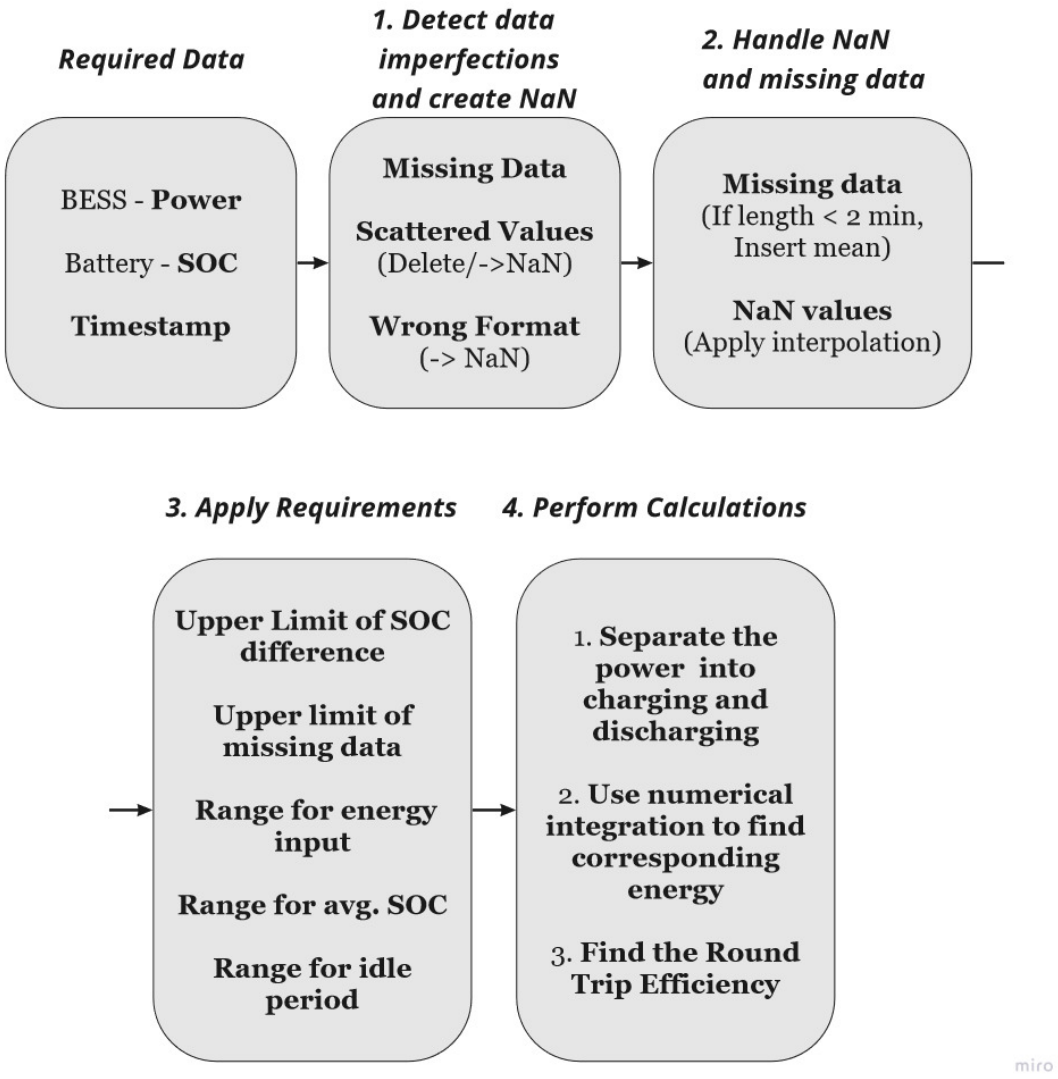

Figure 4.15: Steps to a representative RTE from operational data, including suggest ens for requirement. The specific step used in this study is shown inside the parenthesis.

4.7 Final Discussion

The BESS efficiency was estimated through RTE calculations. Initially, a simple approach was used, followed by a more detailed efficiency analysis. Both the simple RTE calculations and the detailed efficiency analysis exhibited great potential for performance analysis. In order to increase confidence in the results, the methods had to be evaluated for a wider range of data quality and operational conditions. After further analysis, it became clear that in order to obtain consistent results for calculations on operative system efficiency, it is necessary to define certain requirements for BESS behavior and apply them consistently over time. This is because the RTEs will depend on the actual intervals chosen for each requirement, as shown in Table 4.8. Without applying the requirements to identify acceptable and non-acceptable operational be-

havior, the RTE uncertainty increases considerably, resulting in an RTE of 83±5%. However, after incorporating the requirements for the expected operational behavior, less variation in RTE is achieved, with values of 85.5±2.5% and 86.5±1.5% for levels 1 and 2, respectively. Therefore, it is clear that defining and adhering to requirements for a day with expected operations can significantly improve the certainty and consistency of RTE estimations for a BESS.

Additionally, these findings can be used to make a categorization system to distinguish between acceptable and non-acceptable operational days. One example is to create a traffic light system that determines when the BESS is operating under ideal, acceptable, or non-ideal conditions for a specific time period. The system should be trained with historical data to determine the correct intervals for each requirement under different operating conditions. For instance, in this study, ideal conditions could be defined as when the BESS operates within level 2 requirements, acceptable conditions when the BESS operates only within level 1 requirements, and non-ideal conditions when the BESS operates in conditions otherwise and applied at daily intervals. Another implementation is to introduce a grading system post-operation, at the end of each week, where the BESS is graded based on its performance during the week by providing the number of ideal, acceptable, and non-ideal days. For instance, in week 15, the BESS operated under ideal conditions on Days 16 and 17, under acceptable conditions on Days 11 and 15, and under non-ideal conditions on Days 12, 13, and 14, resulting in feedback of 2 ideal days, 2 acceptable days, and 3 non-ideal days. The grading based on requirements in Table 4.8 is consistent with the SOC curves, in Figure 4.6, for each day. The traffic light and grading systems are examples of how to provide the BESS owner with a performance evaluation of the system without disconnecting the BESS physically or operationally.

In order to generalize the suggested approach for calculating BESS efficiency, the method used in this study must be investigated with data from other battery capacities, applications, and battery chemistry. This would enable the determination of other relevant requirements that are essential for those systems and applications, and it would be possible to develop a set of requirements that are relevant for a wide range of BESS sizes and applications. Lastly, since the actual capacity uses similar attributes for its calculation, these findings can provide insight into calculating the parameter through operational data (see Appendix 2).

Conclusion and Further Work

5.1 Conclusion

In an attempt to provide a convenient performance evaluation through BESS efficiency, operational data from a real-life grid-connected PV-BESS system was used. After a thorough investigation of operational data, a strategy for calculating BESS efficiency was proposed, and a traffic light and grading system were suggested for performance evaluation of the BESS. The thesis started with an extensive literature review aimed at identifying the loss mechanisms associated with each subsystem in a BESS, which included the influencing factors C-rate, SOC-range, idle period, input, temperature, and potential inaccuracies in certain parameters such as SOC estimations due to BMS models. Next, operational data was collected and analyzed to compute BESS efficiency in a peak shaving application. Knowledge on the influencing factors of energy loss was applied to gain insights into the performance of the BESS. To ensure consistency, a daily time interval which represented the expected operation was used.

Upon further investigation, it was found that additional requirements for data quality and operational conditions were necessary in order to produce consistent results. Data quality involved dealing with missing data and SOC differences. It was also found that results obtained at aggregated data $>$ 1 minute intervals were significantly inaccurate unless the BESS operated with high input and SOC ranges. Operational conditions depended mainly on the properties of energy input and output, and this study suggested using tools such as energy input, average SOC, and idle period to identify aspects of BESS operation. In the final discussion, two ways of implementing these findings were suggested: a traffic light system to categorize performance, for short periods, as ideal, acceptable, or non-ideal based on the RTE, and a grading system to report the overall performance for longer time intervals.

The objective of this thesis was to investigate an approach for performance evaluation through the use of operational data. Based on its findings, this study suggested a methodology for performance evaluation, which provides a basis for further research

on this topic.

5.2 Further Work

Due to time restrictions and limited available data, several aspects of this research remain unexplored and require further investigation. In order to ensure the reliability and consistency of the results obtained through the system efficiency analysis, the suggested approach has to be applied to similar data with longer time periods. In order to generalize this approach, additional research must be conducted on various sizes of BESS, applications, and technologies.

BMS data, in minute format, would enable a more extensive application of detailed efficiency analysis. In that case, the performance of different subsystems could also be evaluated with more certainty. This could be interesting for fault detection and diagnostics. For example, if the BESS shows bad performance despite ideal apparent conditions, then the detailed efficiency analysis would provide insight into where the BESS is compromising.

Data that includes some information on the power consumption from auxiliary systems would be very helpful in further mapping out the losses in BESS. Alternatively, if the system composition enables information on the properties of auxiliary power consumption, it could be possible to include the related energy losses as a part of the detailed efficiency analysis. The data used in this research was measured in specific weather conditions; it would also be interesting to see how different weather conditions impact the system efficiency calculations.

Bibliography

[1] United Nations. "Take urgent action to combat climate change and its impacts". In: (2015). URL: https://unstats.un.org/sdgs/report/2021/goal-13/.

[2] European Comission. "REPowerEU: affordable, secure and sustainable energy for Europe". In: (2022). URL: https://ec.europa.eu/info/strategy/priorities-2019-2024/european-green-deal/repowereu-affordable-secure-and-sustainable-energy-europe_en.

[3] Ivar Kvaal. "Solution Booklet Positive Energy Districts". In: (2021). URL: https://smart-cities-marketplace.ec.europa.eu/insights/solutions/solution-booklet-positive-energy-districts.

[4] V.Arangarajan et al. "Characteristics and Applications of Energy Storage System to power network - A review". In: (2014). URL: https://researchportal.murdoch.edu.au/esploro/outputs/991005540915907891.

[5] IEA. "Global EV Outlook 2018". In: (2018). URL: https://www.iea.org/reports/global-ev-outlook-2018.

[6] Tsiropoulos I, Tarvydas D, and Lebedeva N. "Li-ion batteries for mobility and stationary storage applications". In: KJ-NA-29440-EN-N (online) (2018). ISSN: 1831-9424 (online). DOI: 10.2760/87175. URL: https://publications.jrc.ec.europa.eu/repository/handle/JRC113360.

[7] Statista. "Size of the global battery market from 2018 to 2021, with a forecast through 2030, by technology". In: (2022). URL: https://www.statista.com/statistics/1339880/global-battery-market-size-by-technology/.

[8] Alasdair J. Crawford et al. "Lifecycle comparison of selected Li-ion battery chemistries under grid and electric vehicle duty cycle combinations". In: *Journal of Power Sources* 380 (2018), pp. 185–193. ISSN: 0378-7753. DOI: https://doi.org/10.1016/j.jpowsour.2018.01.080. URL: https://www.sciencedirect.com/science/article/pii/S0378775318300806.

[9] A.G. Olabi et al. "Critical review of energy storage systems". In: *Energy* 214 (2021), p. 118987. ISSN: 0360-5442. DOI: https://doi.org/10.1016/j.energy.2020.118987. URL: https://www.sciencedirect.com/science/article/pii/S0360544220320946.

[10] Eliseo Zarate-Perez et al. "Battery energy storage performance in microgrids: A scientific mapping perspective". In: *Energy Reports* 8 (2022). Technologies and Materials for Renewable Energy, Environment and Sustainability, pp. 259–268. ISSN: 2352-4847. DOI: https://doi.org/10.1016/j.egyr.2022.06.116. URL: https://www.sciencedirect.com/science/article/pii/S2352484722012598.

[11] Mostafa Rezaeimozafar et al. "A review of behind-the-meter energy storage systems in smart grids". In: *Renewable and Sustainable Energy Reviews* 164 (2022), p. 112573. ISSN: 1364-0321. DOI: https://doi.org/10.1016/j.rser.2022.112573. URL: https://www.sciencedirect.com/science/article/pii/S1364032122004695.

[12] Nathan Blair et al. "Global Overview of Energy Storage Performance Test Protocols". In: (Mar. 2021). DOI: 10.2172/1696786. URL: https://www.osti.gov/biblio/1696786.

[13] "Electrical energy storage (EES) systems - Part 2-1: Unit parameters and testing methods - General specification". In: (Apr. 2018).

[14] Michael Schimpe et al. "Energy efficiency evaluation of a stationary lithium-ion battery container storage system via electro-thermal modeling and detailed component analysis". In: *Applied Energy* 210 (Nov. 2017). ISSN: 0306-2619. DOI: 10.1016/j.apenergy.2017.10.129. URL: https://www.osti.gov/biblio/1409737.

[15] Anna-Lena Lane, Magdalena Boork, and Patrik Thollander. "Barriers, Driving Forces and Non-Energy Benefits for Battery Storage in Photovoltaic (PV) Systems in Modern Agriculture". In: *Energies* 12.18 (2019). ISSN: 1996-1073. DOI: 10.3390/en12183568. URL: https://www.mdpi.com/1996-1073/12/18/3568.

[16] Lazard. "Lazard's levelized cost of storage analysis - version 6". In: (2020). URL: https://www.lazard.com/media/g3jjbcgs/lazards-levelized-cost-of-storage-version-60-vf2.pdf.

[17] Stefan Englberger, Andreas Jossen, and Holger Hesse. "Unlocking the Potential of Battery Storage with the Dynamic Stacking of Multiple Applications". In: (2020). URL: https://www.sciencedirect.com/science/article/pii/S2666386420302563.

[18] NREL. "Analysis of Photovoltaic System Energy Performance Evaluation Method". In: (Nov. 2013). DOI: 10.2172/1111193. URL: https://www.nrel.gov/docs/fy14osti/60628.pdf.

[19] Izumi Kaizuka (RTS Corporation) Gaetan Masson (Becquerel Institute). "TRENDS IN PHOTOVOLTAIC APPLICATIONS". In: (2022). URL: https://iea-pvps.org/trends_reports/trends-2022/.

[20] Tianmei Chen et al. "Applications of Lithium-Ion Batteries in Grid-Scale Energy Storage Systems". In: *Transactions of Tianjin University* 26.3 (June 2020), pp. 208–217. ISSN: 1995-8196. DOI: 10.1007/s12209-020-00236-w. URL: https://doi.org/10.1007/s12209-020-00236-w.

[21] Anupam Parlikar, Holger Hesse, and Andreas Jossen. "Topology and Efficiency Analysis of Utility-Scale Battery Energy Storage Systems". In: (Jan. 2019). DOI: 10.2991/ires-19.2019.15.

[22] Giuliano Rancilio et al. "BESS modeling: investigating the role of auxiliary system consumption in efficiency derating". In: (2020), pp. 189–194. DOI: 10.1109/SPEEDAM48782.2020.9161875.

[23] M.S. Racine, J.D. Parham, and M.H. Rashid. "An overview of uninterruptible power supplies". In: (2005), pp. 159–164. DOI: 10.1109/NAPS.2005.1560518.

[24] Windy Dankoff. "How to Choose an Inverter for an Independent Energy System". In: (2001). URL: https://www.solar-electric.com/lib/wind-sun/Pump-Inverter.pdf.

[25] Haaris Rasool et al. "Optimal Design Strategy and Electro-Thermal Modelling of a High-Power Off-Board Charger for Electric Vehicle Applications". In: (2020). DOI: DOI:10.1109/EVER48776.2020.9242993.

[26] Lydia Dorrmann et al. “Compendium: Li-ion batteries. Principles, characteristics, laws and standards”. In: (Oct. 2021). URL: https://www.dke.de/en/search?q=kompendium&a=blob.

[27] Integer. “Key Battery Terminology”. In: (2022). URL: https://s24.q4cdn.com/142631039/files/doc_presentations/Key-Terminology.pdf.

[28] Naoki Nitta et al. “Li-ion battery materials: present and future”. In: *Materials Today* 18.5 (2015), pp. 252–264. ISSN: 1369-7021. DOI: https://doi.org/10.1016/j.mattod.2014.10.040. URL: https://www.sciencedirect.com/science/article/pii/S1369702114004118.

[29] Battery University. “Types of Lithium-ion”. In: (2021). URL: https://batteryuniversity.com/article/bu-205-types-of-lithium-ion.

[30] Dr Victoria Adesanya-Aworinde. “Electric bus sector is game changer for battery market”. In: (2016). URL: https://www.electricvehiclesresearch.com/articles/9175/electric-bus-sector-is-game-changer-for-battery-market.

[31] CKai-Philipp Kairies. “Battery storage technology improvements and cost reductions to 2030: A Deep Dive”. In: (Mar. 2017). URL: https://www.irena.org/-/media/Files/IRENA/Agency/Events/2017/Mar/15/2017_Kairies_Battery_Cost_and_Performance_01.pdf.

[32] Ronald Dell and Rand D A J. *Understanding batteries*. Royal Society of Chemistry, 2001.

[33] Garche Jurgen. “Encyclopedia of electrochemical power sources”. In: (2009). URL: https://www.sciencedirect.com/referencework/9780444527455/encyclopedia-of-electrochemical-power-sources.

[34] Elena M. Krieger and Craig B. Arnold. “Effects of undercharge and internal loss on the rate dependence of battery charge storage efficiency”. In: *Journal of Power Sources* 210 (2012), pp. 286–291. ISSN: 0378-7753. DOI: https://doi.org/10.1016/j.jpowsour.2012.03.029. URL: https://www.sciencedirect.com/science/article/pii/S0378775312006283.

[35] Kaiyuan Li and King Jet Tseng. “Energy efficiency of lithium-ion battery used as energy storage devices in micro-grid”. In: (2015), pp. 005235–005240. DOI: 10.1109/IECON.2015.7392923.

[36] Evelina Wikner and Torbjörn Thiringer. “Extending Battery Lifetime by Avoiding High SOC”. In: *Applied Sciences* 8.10 (2018). ISSN: 2076-3417. DOI: 10.3390/app8101825. URL: https://www.mdpi.com/2076-3417/8/10/1825.

[37] Ovejas V.J. and Cuadras A. “Effects of cycling on lithium-ion battery hysteresis and overvoltage”. In: (). DOI: https://doi.org/10.1038/s41598-019-51474-5. URL: https://www.nature.com/articles/s41598-019-51474-5#citeas.

[38] V.J. Ovejas and A. Cuadras. “State of charge dependency of the overvoltage generated in commercial Li-ion cells”. In: *Journal of Power Sources* 418 (2019), pp. 176–185. ISSN: 0378-7753. DOI: https://doi.org/10.1016/j.jpowsour.2019.02.046. URL: https://www.sciencedirect.com/science/article/pii/S0378775319301715.

[39] Martin Henke and Getu Hailu. “Thermal Management of Stationary Battery Systems: A Literature Review”. In: *Energies* 13.16 (2020). ISSN: 1996-1073. DOI: 10.3390/en13164194. URL: https://www.mdpi.com/1996-1073/13/16/4194.

[40] Johannes Schmalstieg et al. “From accelerated aging tests to a lifetime prediction model: Analyzing lithium-ion batteries”. In: (2013), pp. 1–12. DOI: 10.1109/EVS.2013.6914753.

[41] Eduardo Redondo-Iglesias, Pascal Venet, and Serge Pelissier. "Global Model for Self-Discharge and Capacity Fade in Lithium-Ion Batteries Based on the Generalized Eyring Relationship". In: *IEEE Transactions on Vehicular Technology* 67.1 (2018), pp. 104–113. DOI: 10.1109/TVT.2017.2751218.

[42] Battery University. "What Causes Capacity Loss?" In: (2021). URL: https://batteryuniversity.com/article/bu-802-what-causes-capacity-loss.

[43] Haiyu Liao et al. "Research on a fast detection method of self-discharge of lithium battery". In: *Journal of Energy Storage* 55 (2022), p. 105431. ISSN: 2352-152X. DOI: https://doi.org/10.1016/j.est.2022.105431. URL: https://www.sciencedirect.com/science/article/pii/S2352152X22014232.

[44] Nashvinder Singh. "ENERGY MANAGEMENT SYSTEM (EMS) ELABORATED". In: (). URL: https://blog.norcalcontrols.net/energy-management-system-ems-ellaborated.

[45] Derek Heeger et al. "Lithium Battery Health and Capacity Estimation Techniques Using Embedded Electronics". In: (Oct. 2017). DOI: 10.2172/1596204. URL: https://www.osti.gov/biblio/1596204.

[46] Essam Ali, Mohamed Fanni, and Abdelfatah Mohamed. "A New Battery Selection System and Charging Control of a Movable Solar-Powered Charging Station for Endless Flying Killing Drones". In: *Sustainability* 14 (Feb. 2022), p. 2071. DOI: 10.3390/su14042071.

[47] Matthew T. Lawder et al. "Battery Energy Storage System (BESS) and Battery Management System (BMS) for Grid-Scale Applications". In: *Proceedings of the IEEE* 102.6 (2014), pp. 1014–1030. DOI: 10.1109/JPROC.2014.2317451.

[48] Rui Xiong. "Battery Management Algorithm for Electric Vehicles". In: (2020), p. 297. URL: https://link.springer.com/book/10.1007/978-981-15-0248-4.

[49] Sofiane Kichou, Nikolaos Skandalos, and Petr Wolf. "Evaluation of Photovoltaic and Battery Storage Effects on the Load Matching Indicators Based on Real Monitored Data". In: *Energies* 13.11 (2020). ISSN: 1996-1073. DOI: 10.3390/en13112727. URL: https://www.mdpi.com/1996-1073/13/11/2727.

[50] Jinpeng Tian, Rui Xiong, and Weixiang Shen. "A review on state of health estimation for lithium ion batteries in photovoltaic systems". In: *eTransportation* 2 (2019), p. 100028. ISSN: 2590-1168. DOI: https://doi.org/10.1016/j.etran.2019.100028. URL: https://www.sciencedirect.com/science/article/pii/S2590116819300281.

[51] Feng Leng, Cher Tan, and Michael Pecht. "Effect of Temperature on the Aging rate of Li Ion Battery Operating above Room Temperature". In: *Scientific reports* 5 (Aug. 2015), p. 12967. DOI: 10.1038/srep12967.

[52] Robert Camilleri and Mahmoud Sawani. "PREDICTING THE TEMPERATURE DISTRIBUTION IN A LITHIUM ION BATTERY CELL FOR DIFFERENT COOLING STRATEGIES". In: (Sept. 2019). DOI: 10.13140/RG.2.2.15461.76006. URL: https://www.researchgate.net/publication/335716756_PREDICTING_THE_TEMPERATURE_DISTRIBUTION_IN_A_LITHIUM_ION_BATTERY_CELL_FOR_DIFFERENT_COOLING_STRATEGIES?channel=doi&linkId=5d7793fd4585151ee4ab4acb&showFulltext=true.

[53] Taeyoung Han, Bahram Khalighi, and Shailen Kaushik. "Li-ion Battery Thermal Management – Air vs. Liquid Cooling". In: (Jan. 2017), pp. 1309–1322. DOI: 10.1615/TFEC2017.fna.017297.

[54] Nasima Tamboli. "Effective Strategies for Handling Missing Values in Data Analysis (Updated 2023)". In: (Oct. 2021). URL: https://www.analyticsvidhya.com/blog/2021/10/handling-missing-value/.

[55] Md Dhali, Farhad Bulbul, and Umme Sadiya. "Comparison on Trapezoidal and Simpson's Rule for Unequal Data Space". In: *International Journal of Mathematical Sciences and Computing* 5 (Nov. 2019), pp. 33–43. DOI: 10.5815/ijmsc.2019.04.03.

[56] Elena. "Comparing Numerical Integration Methods". In: (Feb. 2015). URL: https://codefying.com/2015/02/10/comparing-numerical-integration-methods/.

[57] DNV. "2020 BATTERY PERFORMANCE SCORECARD". In: (2020). URL: https://www.dnv.com/Publications/2020-battery-performance-scorecard-192180#.

[58] Nicholas DiOrio et al. "Technoeconomic Modeling of Battery Energy Storage in SAM". In: (Sept. 2015). DOI: 10.2172/1225314. URL: https://www.osti.gov/biblio/1225314.

[59] Yuanyuan Shi et al. "A Convex Cycle-based Degradation Model for Battery Energy Storage Planning and Operation". In: (Mar. 2017). URL: https://ieeexplore.ieee.org/document/8431814.

[60] Valentin Silvera Diaz et al. "Comparative Analysis of Degradation Assessment of Battery Energy Storage Systems in PV Smoothing Application". In: *Energies* 14.12 (2021). ISSN: 1996-1073. DOI: 10.3390/en14123600. URL: https://www.mdpi.com/1996-1073/14/12/3600.

Appendix 1

6.1 Overview on RTE, SOC difference, Energy Input, Energy Output

Day	RTE[%]	SOC diff[%]	Energy In[kWh]	Energy Out[kWh]
5	86.92	0.37	23.54	20.46
6	84.66	0.33	6.69	5.67
7	83.31	-1.07	5.88	4.90
8	87.02	0.71	12.34	10.74
9	78.92	-0.04	4.73	3.73
10	84.71	-0.23	16.25	13.77
11	85.33	0.70	17.59	15.01
12	80.27	0.17	7.05	5.66
13	0.00	-3.29	0.00	0.00
14	12.59	0.86	0.96	0.12

Table 6.1: Contains RTE, SOC difference, Input and Output for days 5-14.April, based on values from minute data.

Appendix 2

7.1 Actual Capacity - Results

Although the primary objective of this analysis is to develop an understanding of RTE calculations, the calculation of actual capacity involves similar concepts and principles. An introduction to the actual capacity parameter, and insights into its calculation, may have potential benefits for future analyses. To determine the actual capacity from operational data, two critical components are required: the maximum DOD and the associated energy. While the energy can be obtained by simple numerical integration, the main challenge is finding the corresponding indexes for the DOD. Therefore, this section focuses on the approaches for determining the DOD. Specifically, two different methods are described: the first involves manually looping through the SOC curve to identify the required DOD, while the second involves utilizing rain flow counting to identify distinct cycles. It is important to note that the following calculation does not rely on BMS data, and thus Set1 will be used for this purpose.

7.1.1 Method 1: Finding DOD Manually

This algorithm searches through the data to find two points where the DOD is as large as possible. The results for day 10 are shown in 7.1.

The maximum DOD for day 10 is approximately 72%. The algorithm identified a total of 120 points where the DOD is approximately 72%, with a precision of two decimals. The estimated actual capacity of the BESS is 12.5±1 kWh. The SOC curves indicate an expected maximum DOD of 75%, but it appears that the EMS limited the maximum DOD to 72% to account for standby losses and prevent the need for dependency on the grid. With respect to the methodology, it will provide outcomes with the highest possible accuracy. However, the computational time may present a challenge when handling larger input data, which may be necessary for tracking the actual capacity over an extended period of time. This issue is already apparent, as the computation time for a single day amounts to approximately 0.15 seconds.

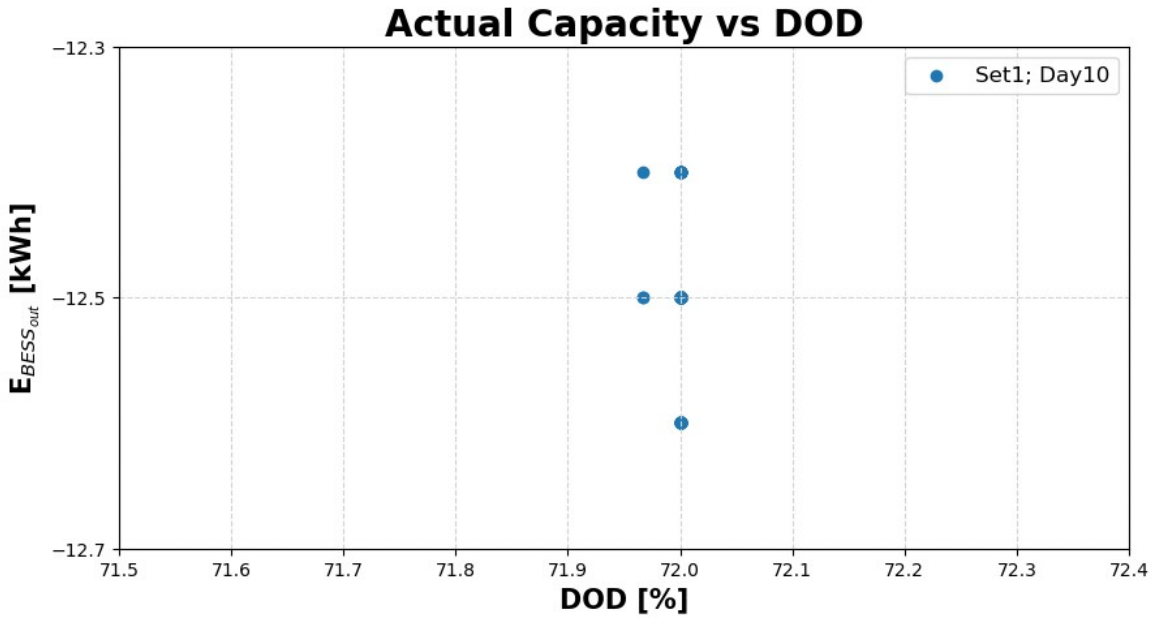

Figure 7.1: The maximum $E_{BESS_{out}}$ and the maximum DOD, which represent the actual capacity of BESS for 2022-04-10.

7.1.2 Method 2: DOD through Rainflow Counting

The rain flow counting method utilizes a similar underlying principle to 'method 1'; however, it incorporates a cycle division process within its algorithm, which corresponds to the respective ranges of the curve. When applying this algorithm to the SOC curve, the ranges will represent the DOD. Rain flow counting was applied on day 10, and the results can be seen in Figure 7.2. The algorithm divided the SOC curve for day 10 into 7 cycles, where only two cycles were above 70 % DOD: one cycle when the BESS is charging and one when it's discharging. The discharge cycle was equal to a DOD of approximately 72%. According to the result, the actual capacity of 72% DOD is 12.5kwh with a computation time of approximately 0.05 s.

The estimated actual capacity derived from rain flow counting was found to be equivalent to the mean actual capacity estimated from the first method. While the computational time required by this method is considerably shorter, it has the drawback of automatically rounding up the SOC value. To obtain outcomes with greater decimal precision, the values must be manually extracted from the original data by utilizing the appropriate interval for the maximum DOD range. According to [60], the rainflow counting method is effective at identifying small DOD, but it may not perform as well for identifying cycles in higher DOD, which can limit its usefulness for finding the actual capacity.

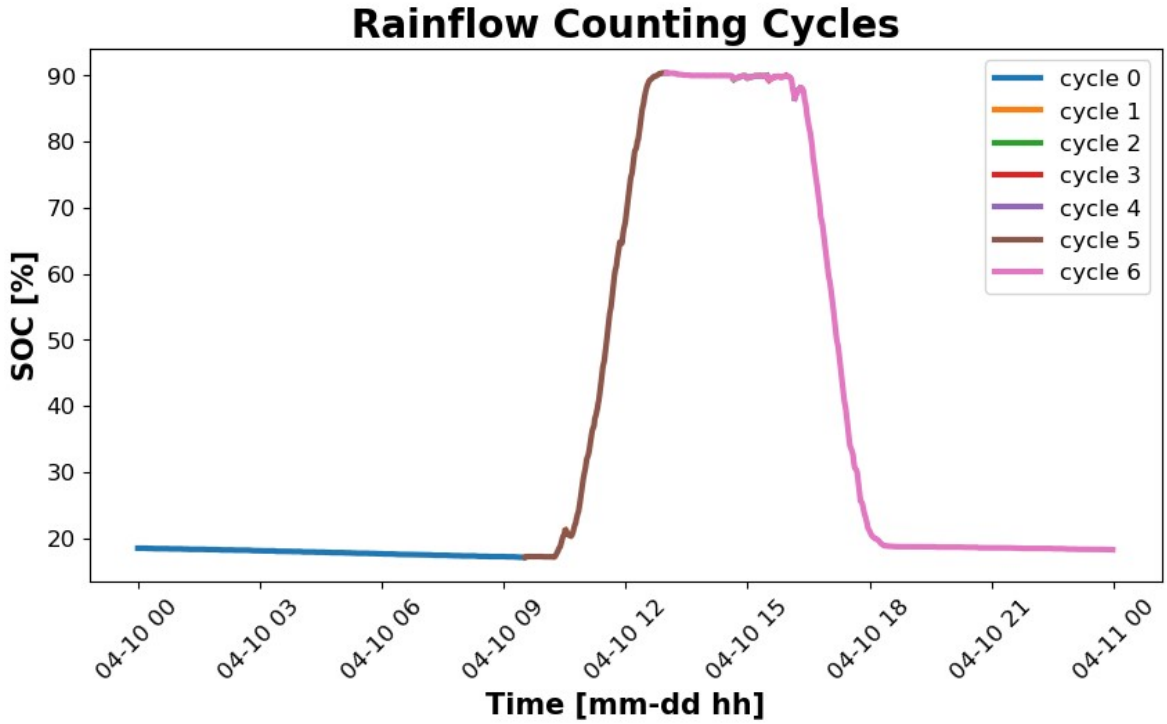

Figure 7.2: The SOC curve for 2022-04-10 was divided into different DODs according to the rain flow counting method.

7.1.3 Weekly Mean Value of Actual Capacity

When utilizing operational data for capacity estimation, it is crucial to take into account the various factors that influence the results. To gain a more comprehensive understanding of the potential variation in outcomes, rain flow counting was performed on each day of the weeks in April 2022 where the discharged DOD is approximately 72%, ensuring that the conditions are as similar as possible. The results of this analysis are depicted in Figure 7.3. Weeks 14 and 15 had only two days each with the

Day	5	10	16	17	19	20	21	23	24	28	29
Average SOC[%]	35	45	51	53	57	55	54	39	49	36	54

Table 7.1: The average SOC for each discharge cycle.

requested DOD of $\approx$ 72%. The actual capacity in Week 14 was approximately 12.5 kWh, whereas Week 15 had a higher actual capacity of 12.7 kWh. Week 16 had the highest number of viable days, and the actual capacity varied the most, with a mean discharge energy of 12.7 kWh. Week 17 had only two days with a mean actual capacity of 12.2 kWh, which is smaller than the previous weeks. A box plot summarizing the weekly results is presented in Figure 7.4, which provides a better overview of the results shown in Figure 7.3.

Assuming that the battery has insignificant capacity fade is a reasonable assump-

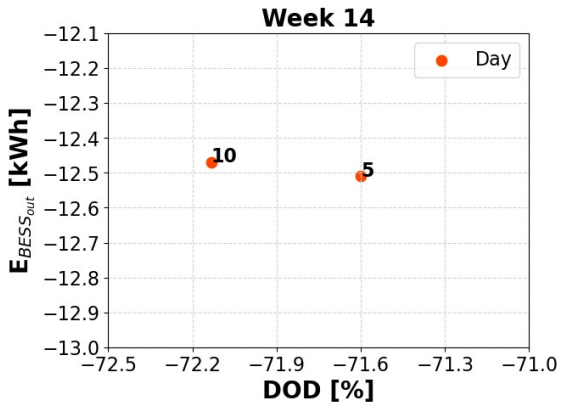

(a) Actual capacity for week 14 is [-12.47,-12.51]

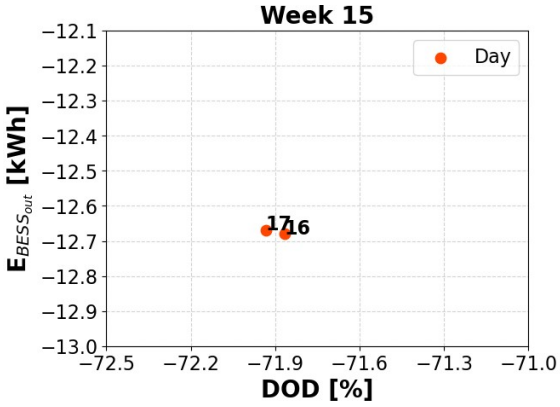

(b) Actual capacity for week 15 is [-12.67,-12.68]

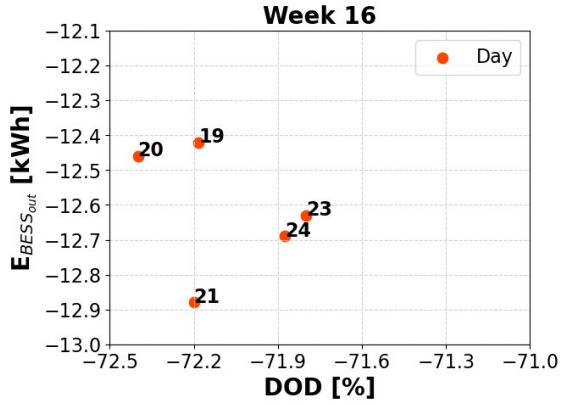

(c) Actual capacity for week 16 is [-12.42,-12.88]

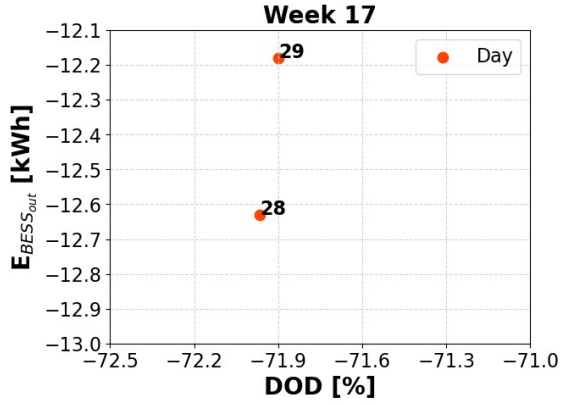

(d) Actual capacity for Week 17 is [-12.18,-12.63]

Figure 7.3: The actual capacity is ≈ 72% DOD, which was found by using the rain flow counting method. Four figures represent the four weeks in April 2022. Each week includes days when the BESS operation reached the maximum DOD of 72%. Each point is labeled with a day and average SOC for the relevant time period.

tion for this battery, which has not been used extensively; therefore, for the following estimation of the actual capacity, the nominal capacity from the data sheet is used. For a 72% DOD and an 85% RTE, the expected actual capacity of BESS is 19.56kWh×0.72 × 0.85 ≈ 12kWh. The mean actual capacity of the BESS during the month of April, as depicted in Figure 7.4, was found to be 12.5 ± 0.2 kWh. The observed differences in the actual capacity on different days are not necessarily attributed to the intrinsic properties of the BESS. Diverse factors, as previously discussed, cause variations in operation during discharge that are reflected in the average SOC and p-rate. Additionally, the accuracy of the DOD could also account for the inconsistent results. Since the p-rates are very low, the focus will be on the average SOC and the DOD accuracy.

Based on the result, most days provide an actual capacity of around 12.5 kWh. The

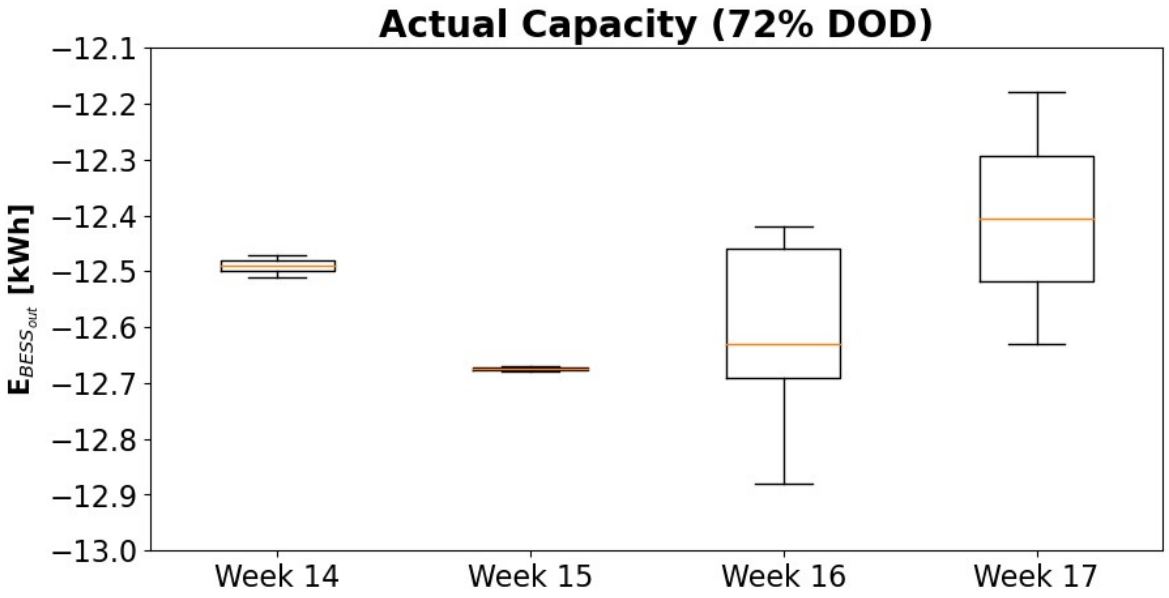

Figure 7.4: Box plot that summarizes the estimated actual capacity for DOD ≈ 72% for each week in April 2022.

exceptional cases are day 21, with a high actual capacity of 12.9 kWh, and day 29, with a low actual capacity of 12.1 kWh. When examining Figure 4.11 both have the same energy input throughout the day. However, Figure 4.12 shows that the p-rate during discharge for day 29 is slightly lower, and Figure 4.14 shows that the p-rate is mainly different in the idle period. Day 29 has an idle period of 15, which indicates that it has a longer operating period with more fluctuations in the SOC curve. Days 19, 20, and 21 all have similar average SOC and DOD accuracy; however, day 21 is unexpectedly high, which indicates that there are other factors that play a role in the accuracy of actual capacity. One observable difference is that day 21 has a 2 kWh higher energy input than the other days, which also means that, given similar losses, it will have more energy discharged.

7.1.4 Takeaways for Further Analysis

The actual capacity showed promising results. Although there were some inconsistencies within the week, the mean values showed small uncertainties; see Figure 7.4.Similar to RTE, the actual capacity is influenced both by data quality issues related to the accuracy of DOD and by operational conditions.

The same conditions for data handling apply: missing data, resolution, and general data qualities. The methodologies used to determine the actual capacity of a BESS are dependent on the quality of the discharged energy, which can be influenced by various operational factors such as the C-rate, fluctuations in the discharged energy,

and the quality of the data obtained. For further analysis, the following investigations are recommended: the accuracy of the SOC value. The relationship between the SOC and power curve and how the handling of missing data and NaN values may impact the final accuracy Since it is expected that the C-rate will have a great influence on capacity and health estimations, BMS data is also relevant.

The actual capacity can be used for the health estimation of the BESS. By tracking the actual capacity over time, it should provide insight on potential capacity fade. Although the results presented acceptable accuracy, it was not possible to identify specific factors responsible for the inconsistencies observed. In order to gain greater confidence in using this approach for the potential health estimation of the BESS, further investigation is required. After developing confidence in the actual capacity calculations, the main objective should be to determine if they can be utilized to monitor the health of BESS over an extended period of time, which would require a dataset with a significantly longer time period.